جامعة الأمير سطام بن عبدالعزيز
PRINCE SATTAM BIN ABDULAZIZ UNIVERSITY
College of Engineering
Mechanical Engineering Department

Innovation and Technology

Pride of today and the future of tomorrow

The official magazine for graduation projects of Mechanical Engineering Department

Volume 1, 23-24

Editorial Team

About Innovation and Technology

Aims & Scope

Innovation & Technology is the official magazine for projects of the Mechanical Engineering Department. It aims to publish state-of-art knowledge in the following fields:

1-**Thermodynamics and Heat Transfer:** Studies on energy conversion, heat exchangers, refrigeration, and thermal management.

2-**Fluid Mechanics and Hydraulics:** Research on fluid behavior, fluid-structure interaction, and hydraulic systems.

3-**Materials Science and Engineering:** Investigations into material properties, composites, nanomaterials, and material manufacturing processes.

4-**Solid Mechanics and Structural Analysis:** Analyses of stress, strain, elasticity, plasticity, fracture mechanics, and structural stability.

5-**Manufacturing and Production Engineering:** Focus on manufacturing processes , automation, additive manufacturing, and production optimization.

6-**Robotics and Mechatronics:** Studies on robotic systems, control theory, sensors, actuators, and intelligent systems.

7-Dynamics and Control: Studies on the behavior of mechanical systems, vibration analysis, control systems, and kinematics.

8-**Mechanical Design and CAD/CAM:** Innovations in mechanical design,computer-aided design (CAD), computer-aided manufacturing (CAM), and product lifecycle management.

9-**Automotive and Aerospace Engineering:** Studies on vehicle dynamics, propulsion systems, aerodynamics, and aerospace structures.

10-**Biomechanics and Biomedical Engineering:** Studies on the application of mechanical principles to biological systems, medical devices, and prosthetics.

11-**Energy Systems and Renewable Energy:** Investigations into power generation, renewable energy technologies, energy storage, and energy efficiency.

12-Tribology and Surface Engineering: Studies on friction, lubrication, wear, and surface treatments to enhance material performance.

Innovation & Technology magazine offers an online platform facilitating the effective exchange of innovative scientific and engineering ideas and the dissemination of recent, original, and significant research and developmental findings

Contents

Design and Manufacture a New Prototype of a Corrugated Convex Shape Absorber Solar Still for Water Desalination

Fahad Alotaibi[1], Faisal Alrwuais[2], Abdelkader Abdullah[3], Umar Alqsair[4]

Department of Mechanical Engineering, College of Engineering in Al-Kharj, Prince Sattam bin Abdulaziz University, Al-Kharj 11942, Saudi Arabia

[1] 441050383@std.psau.edu.sa; [2] 441051579@std.psau.edu.sa; [3]a.abdullah@psau.edu.sa;[4] u.alqsair@psau.edu.sa

***Abstract*:** Solar stills, the most fundamental technology for harnessing solar energy for freshwater acquisition, utilize a straightforward process. Sunlight directly evaporates fresh water from seawater or brackish water sources. This study investigated the potential for augmenting solar stills' productivity and thermal performance. To achieve this objective, a novel design, the V-corrugated absorber solar still (VCASS), was employed. The V-corrugated absorber serves the dual purpose of significantly increasing the surface area dedicated to evaporation while concurrently reducing the thickness of the brine layer. This innovative design resulted in a remarkable enhancement in freshwater production. The VCASS achieved a superior freshwater productivity of 5863 mL/m². day, surpassing the conventional solar still's (CSS) output of 1538 mL/m². day by a staggering 281%. These findings not only demonstrate the efficacy of the V-corrugated absorber design in enhancing solar still performance but also offer a promising avenue for further development in clean water production technologies, particularly in regions with limited access to freshwater resources. The implementation of VCASS technology has the potential to provide a sustainable and efficient solution for addressing global water scarcity challenges.

Keywords: desalination, solar energy, solar still, v-corrugated absorber, phase change material.

1. INTRODUCTION

The scarcity of fresh water is a growing global challenge, particularly in arid and semi-arid regions [1]. Desalination technologies offer a promising solution to address this issue. Among them, solar stills present a sustainable and low-energy approach for water desalination, utilizing solar energy to evaporate saline water and condense the clean vapor.

However, conventional solar stills often suffer from limitations in efficiency. This research project aims to overcome these limitations by developing a novel prototype: a corrugated convex shape absorber solar still. This design incorporates two key features:

Corrugated Absorber: The corrugated surface area increases solar energy absorption compared to a flat plate, enhancing water evaporation rates.

Convex Shape: The convex shape concentrates incoming sunlight onto the absorber, further amplifying the solar energy capture and thermal efficiency.

This project investigates this innovative solar still prototype's design, fabrication, and performance evaluation. We anticipate that the corrugated convex shape absorber will significantly improve water production compared to traditional solar stills. The successful development of this prototype could contribute significantly to advancing sustainable desalination technologies, particularly in regions with abundant solar resources and limited access to fresh water.

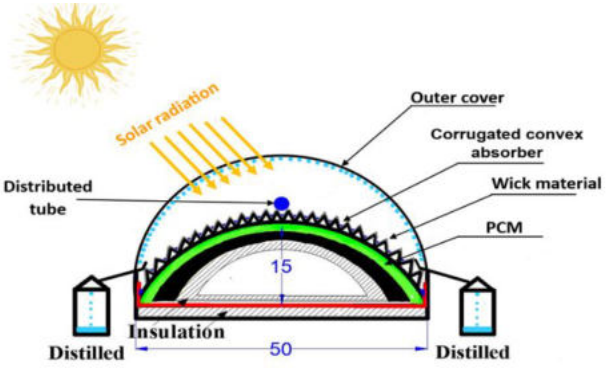

Fig. 1. Schematic diagram of tubular solar still with v-corrugated absorber.

A beacon of hope emerges from solar desalination in arid regions with abundant sunshine. This environmentally friendly technology harnesses the Gulf's potent solar energy (reaching 2400 kW/m²) to transform seawater into life-sustaining freshwater. Through advanced evaporative and condensation processes, solar desalination offers a sustainable and cost-competitive solution to water scarcity. [2]

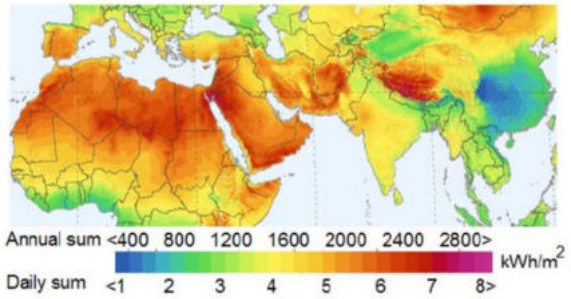

Fig. 2. Solar radiation distribution over the Middle East region [2]

Thus, the objectives of this project based on the above discussion are to investigate a compact solar design with a V-shaped corrugated absorber to significantly increase freshwater production, improve efficiency, and reduce heat loss.

2. V-Corrugated Absorber Design

The core component of this solar still is the V-corrugated absorber, which is crucial for desalination. This innovative design features a V-shape that significantly increases its surface area compared to traditional flat-plate absorbers. This expanded area effectively captures more incoming solar radiation, which is then transferred to the saline water within the basin. The chosen material for the V-corrugated absorber is cold-rolled steel, ensuring compatibility with the final design and offering superior advantages. This combination of increased surface area and optimal material selection maximizes sunlight absorption for efficient water evaporation.

3. V-Corrugated Absorber Solar Still

The meticulous fabrication of each component – the V-corrugated absorber, freshwater collection basin, polycarbonate cover, and wooden base – culminated in a final assembly stage precisely integrated into a functional solar energy collection system. This process involved careful adherence to a pre-defined assembly plan to ensure proper alignment and secure attachment of each element. The comprehensive design and implementation of the V-corrugated absorber system ensured its optimal functionality, culminating in exceptional solar energy collection efficiency.

Fig. 3. V-Corrugated absorber solar still prototype.

4. Experimental Work

The experiment tested a new solar still design (VCASS) in a natural setting at Prince Sattam bin Abdulaziz University in Al-Kharj on May 9th, 2024, from 8 AM to 4 PM. The focus was on how well the VCASS captured sunlight and produced freshwater compared to a traditional design (CSS) under identical conditions. Data on solar radiation, temperatures, and freshwater output was collected throughout the day.

5. Results and Discussion

V-corrugated absorber solar still (VCASS) significantly outperformed the conventional solar still (CSS) in freshwater production (5863 mL/m². day vs 1538 mL/m². day). This is due to the VCASS's increased surface area, improved heat transfer, and enhanced convection.

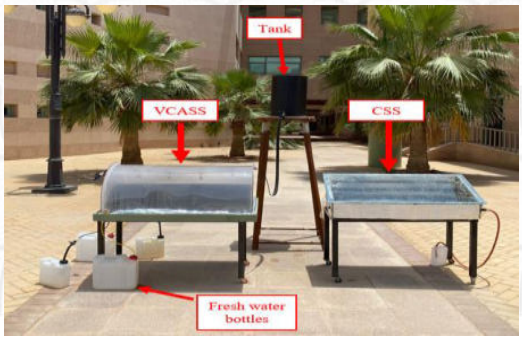

Fig. 4. Experiment Setup

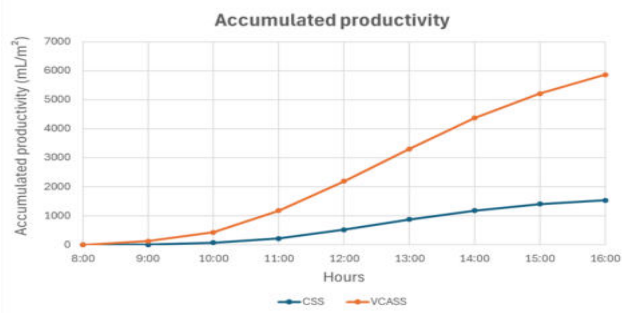

Fig. 5. Accumulated productivity graph for CSS and VCASS.

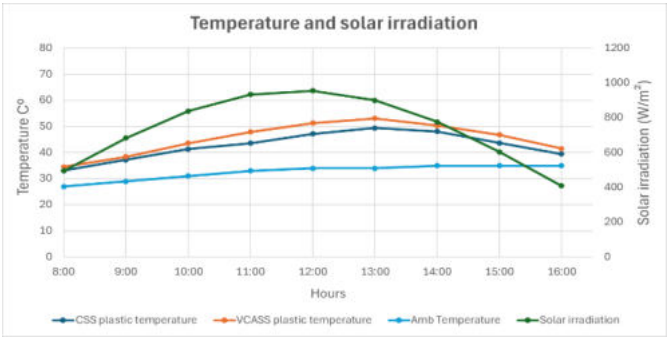

Fig. 6. Temperature and solar irradiation graph for CSS and VCASS

CONCLUSIONS

Experiments conducted with a V-corrugated absorber solar still (VCASS) yielded significant results. The VCASS demonstrated a 281% increase in freshwater production compared to the conventional solar still. This improvement is attributed to its novel design, which enhances evaporation and heat transfer processes. The research underscores the efficacy of geometric modifications in optimizing solar still performance, with the VCASS achieving a daily efficiency of 37.13%, markedly surpassing the 9.74% efficiency of the conventional still. Future research can explore the (VCASS) performance under varying conditions and optimize its design for even better efficiency.

REFERENCES

[1] Unesco, World Water Assessment Programme (United Nations), and UN-Water, Leaving no one behind : the United Nations World Water Development Report 2019.

[2] Mohamed Sabry, Mouaaz Nahas, Saud H. Al-Lehyani. Simulation of a Standalone, Portable Steam Generator Driven by a Solar Concentrator. Energies 8 (2015) 3867-388. doi:10.3390/en8053867.

Green Manufacturing for Fabricating Environmentally Friendly Products

Abdulhadi Baskran[1], Rayan Alzuayr[2], Ali Abd El-Aty[3], Bandar Alzahrani[4], Mohamed Zaky[5]

Department of Mechanical Engineering, College of Engineering in Al-Kharj, Prince Sattam bin Abdulaziz University, Al-Kharj 11942, Saudi Arabia

[1] 441050316@std.psau.edu.sa; [2] 441050671@std.psau.edu.sa; [3] a.hassibelnaby@psau.edu.sa, [4] ba.alzahrani@psau.edu.sa , [5] moh.ahmed@psau.edu.sa

***Abstract*:** This project focuses on implementing green manufacturing practices to fabricate environmentally friendly tiles using recycled tires. The objective is to design and optimize the manufacturing process to produce high-quality tiles while minimizing environmental impact. The effects of temperature, pressure, and holding time on the production process were explored through systematic experimentation with molds of varying sizes. After rigorous testing, the optimal parameters were determined: a pressure of 5 tons at 350°C for 60 minutes. This resulted in the production of durable tiles that meet environmental and performance standards. The success of this project not only demonstrates the feasibility of repurposing discarded tires but underscores the potential of green manufacturing in promoting sustainability and responsible resource management. There are opportunities for further optimization and expansion, including scaling up production. Overall, this project exemplifies the intersection of innovation, sustainability, and social responsibility, showcasing the transformative potential of green manufacturing practices.

Keywords: tires upcycling, green manufacturing, Rubber tiles, mold development, environmentally friendly product.

1. Introduction

Saudi Arabia confronts a critical challenge in effectively managing the surge in waste volume, primarily originating from vehicles and industries, and is expected to escalate with a projected population of 35 million by 2030. The absence of efficient waste management strategies, mainly for automotive waste and industrial by-products, severely threatens environmental sustainability and public health. This pressing issue is exacerbated by the absence of structured recycling programs, innovative technologies, and regulatory frameworks, intensifying environmental degradation through air and water pollution, soil contamination, and increased proliferation of disease vectors. The urgent need for a comprehensive solution is underscored by the current lack of green manufacturing principles, leading to detrimental consequences for the Kingdom's ecological balance and the well-being of its populace.

As shown in Fig. 1, the previous studies of GTs focused on sustainable technologies, environmental technologies, adverse effects of traditional manufacturing technologies, and green investments concerning firm performance. Research on GT adoption is gradually gaining traction as a potential solution for a better environment. This shift is attributed to the heightened public awareness regarding environmental quality, making the outdated "treatment after pollution" approach obsolete. Furthermore, enhancing the sustainability of manufacturing technologies could contribute to stainable development, a phenomenon currently lacking in existing manufacturing practices [1]. Also, Figure 2 shows that most countries focus on green technology, and unfortunately, Saudi Arabia has low efforts [2]

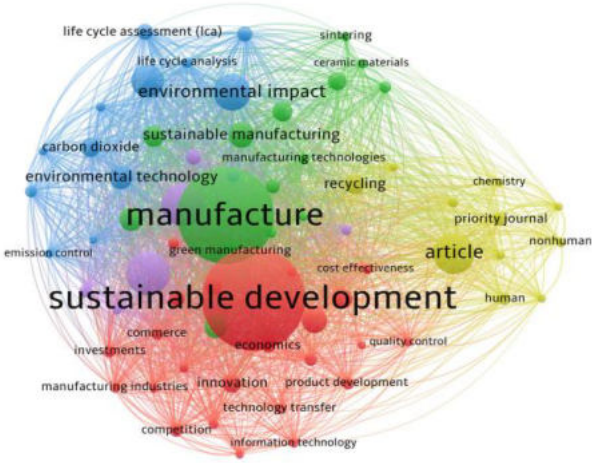

Fig. 1. VOS diagram for the most related topics in GTs [1].

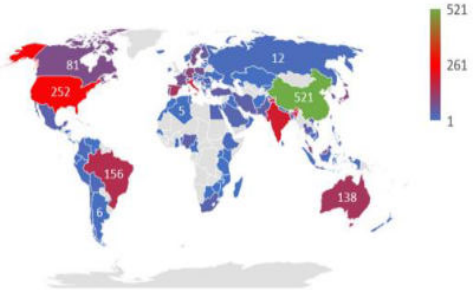

Fig. 2. The most countries focusing on green technology [1]

Thus, the objectives of this project based on the aforementioned discussion are to implement green manufacturing to fabricate environment-friendly products (tiles) from recycled tires, propose a detailed design of the mold used to fabricate environment-friendly tiles and determine the optimum process parameters to manufacture the environment-friendly tiles.

2. Experimental Work

We visited Ahmed Hammoud Al-Jawir for rubber production in Riyadh to gain first-hand insight into their manufacturing process. Figure 3 illustrates the recycling process used in this

project. This study used rubber powder (less than 1 mm) and coarse size (1-5 mm).

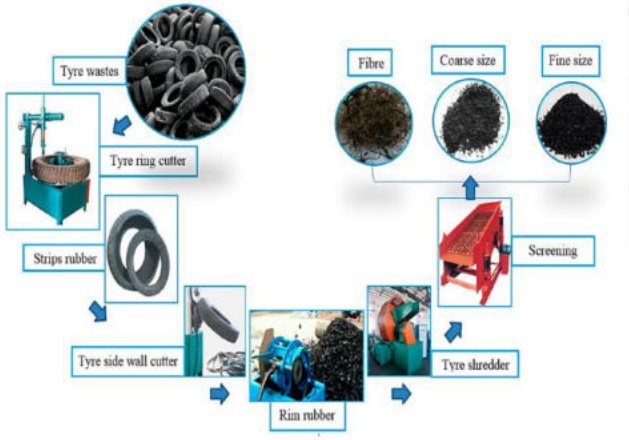

Fig. 3. The stage of recycling the rubes at ambient temperature.

Fabricating environmentally friendly tiles from recycled tires is essential in designing and manufacturing the model and the ejection mechanisms. Mold design is crucial for making things precisely, like in the compression molding process. It's all about creating molds that match the product perfectly. But even with a great mold, you need a good ejection mechanism to get the product out smoothly and safely for the part and the operator. The project aims to improve both aspects to make manufacturing easier and products better.

2.1. Design and Finite element (FE) analysis of the mold.

During the design phase, we developed three concepts with distinct approaches until we reached the final design, as depicted in Fig. 4, where Figs. 4a and b describe the final designs and FE analysis of the proposed environmentally friendly tiles. Comprehensive simulations of the proposed mold designs were accomplished to meticulously analyse stress distribution and ascertain its compliance with our specifications.

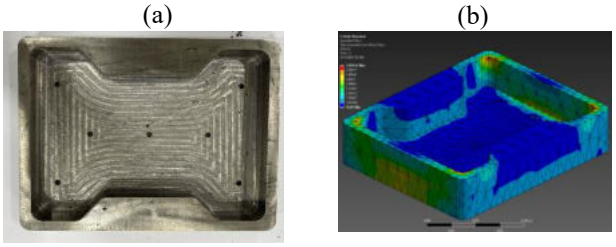

Fig. 4. The mold's initial and final design and FE analysis.

2.2. Design and FE analysis of Ejection mechanism.

The ejection mechanism employs a sophisticated scissors mechanism to facilitate efficient ejection. This mechanism comprises several key components, including an ejection plate, ejection pins, an upper plate, a lower plate, and links. Each component plays a crucial role in the smooth operation of the ejection process. Fig. 5 provides a comprehensive overview of how these elements form the assembly coupling with FE analysis, ensuring optimal functionality and reliability.

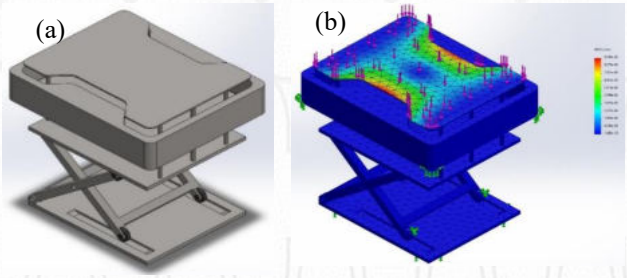

Fig. 5. The design and FE analysis of the Ejection mechanism

3. RESULTS AND DISCUSSION

After completing previous experiments and finite element analysis on the final mold design, we commenced experimental trials with the following parameters: applying pressure ranging from 2 to 5 tons, accompanied by holding times varying from 20 to 60 minutes. The mold was filled with fine rubber powder up to the brim to ensure consistent testing conditions, as depicted in Fig. 6. These experiments aim to investigate the effects of varying pressure levels systematically and holding times on the molding process and the resultant part quality. By meticulously controlling these parameters, we seek to optimize the manufacturing process and achieve the desired characteristics in the molded parts.

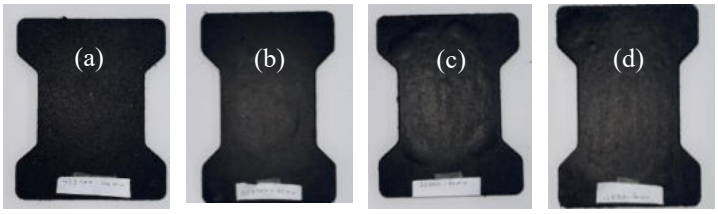

Fig. 6. The tiles are manufactured from recycled tires at a working temperature of 350 °c, and (a)2 tons for 20 mins., (b) 3 tons for 20 mins., (c) 4 tons for a holding time of 60 mins., and (d) 5 tons for a holding time of 60 mins.
temperature 350c

4. CONCLUSIONS

We successfully produce environmentally friendly products by applying green technologies in manufacturing, which resulted in the design, analysis, and manufacturing of a mold and an ejection system.

REFERENCES

[1] Ahn, S.H., 2014. An evaluation of green manufacturing technologies based on research databases. International Journal of Precision Engineering and Manufacturing - Green Technology 1, 5–9. doi:10.1007/s40684-014-0001-8.

[2] Kong, T., Feng, T., Ye, C., 2016. Advanced manufacturing technologies and green innovation: The role of internal environmental collaboration. Sustainability (Switzerland) 8. doi:10.3390/su8101056

Design and Simulation of a Friction Stir Spot Welding Machine

Sohib Zaki[1], Abdulmajed Alharbi[2], Mohamed Zaky[3], Kamel Touileb[4], Bandar Alzahrani[5], Ali Abd El-Aty[6]

Department of Mechanical Engineering, College of Engineering in Al-Kharj, Prince Sattam bin Abdulaziz University, Al-Kharj 11942, Saudi Arabia

[1] 441052055@std.psau.edu.sa; [2] 441050392@std.psau.edu.sa; [3] moh.ahmed@psau.edu.sa, [4] k.touileb@psau.edu.sa, [5] ba.alzahrani@psau.edu.sa , [6] a.hassibelnaby@psau.edu.sa

***Abstract*:** This project focuses on designing and simulating a Friction Stir Spot Welding (FSSW) machine intended explicitly for welding lightweight metals. Drawing inspiration from existing models. The design emphasizes cost-effectiveness without compromising functionality. Detailed specifications consider material compatibility and operational requirements, ensuring optimal performance. Through thorough simulation and refinement, the final machine achieves enhanced weld consistency, increased throughput, and greater versatility while remaining economically viable.

Keywords: Design, Simulation, FSSW Machine, Lightweight Metals, Welding, Cost-effectiveness.

1. Introduction

The demand for lightweight structures is driven by environmental awareness, economic factors, and performance needs. Industries are actively seeking strong yet lightweight materials to create efficient and sustainable products. This has increased the demand for metals like aluminum, magnesium, and titanium. However, welding these metals poses significant challenges due to their unique properties, such as high thermal conductivity and low melting points, which can lead to premature melting or distortion during welding [1]. Quick oxide formation and susceptibility to defects like porosity and cracking further complicate welding operations [2].

To address these challenges, alternative welding methods, such as friction stir spot welding (FSSW), are employed. FSSW operates in a solid state, avoiding issues related to melting and the formation of solidified microstructures. It has proven effective in joining lightweight metals and robust materials like steel and is widely applied in the aerospace and automotive industries [2].

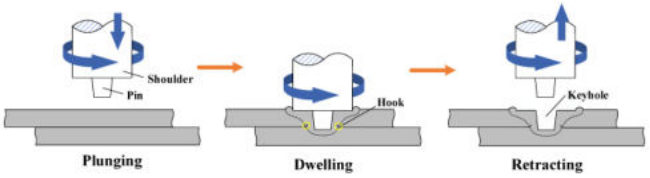

Figure 1, Friction stir spot welding process [2].

2. Experimental Work

The experimental work for designing and simulating a Friction Stir Spot Welding (FSSW) machine aims to address the challenges associated with welding lightweight metals such as aluminum, magnesium, and titanium. The project is structured in several key stages to ensure a comprehensive approach.

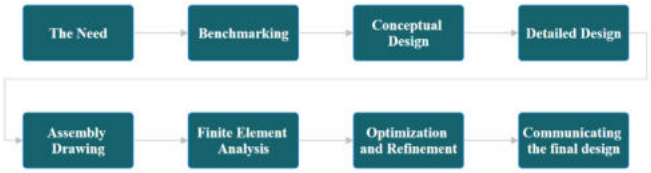

Figure 2, Design Methodology.

2.1. Design Parameters

The design process for the FSSW machine involved a thorough analysis of various factors to ensure the machine meets the required specifications and performs optimally. Key design parameters include functionality, material compatibility, operational requirements, and mechanical design constraints.

2.1.1. Functionality

The primary function of the FSSW machine is to join lightweight metal components through a solid-state welding process. The machine is designed to perform precise and reliable welds by combining rotational speed and axial force to generate frictional heat at the weld interface. The design includes critical components such as the spindle, bearings, slider mechanism, and ball screw assembly, each tailored to support the welding process.

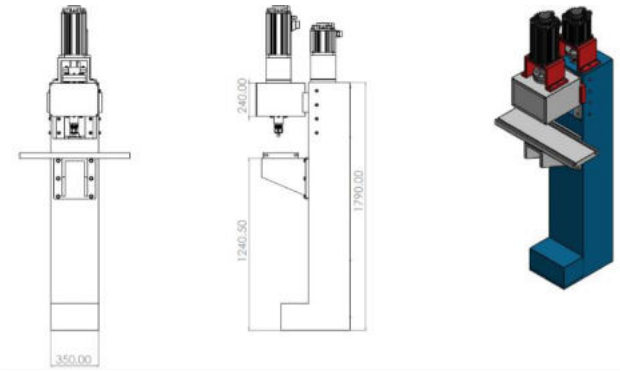

Figure 3, Design of the Machine.

2.1.2. Material Compatibility

Selecting suitable materials for the machine components is crucial to ensure durability and compatibility with the welded metals. The materials chosen for the spindle shaft, bearings, and other critical components can withstand the operational stresses and temperatures
involved in the FSSW process. Using high-strength alloys and advanced composites ensures that the machine

components maintain their integrity and performance over extended periods of use.

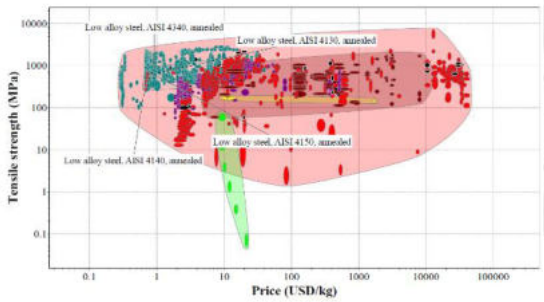

Figure 4, Ashby Plot: Tensile Strength vs. Cost.

2.1.3. Operational Requirements

The operational requirements of the FSSW machine include achieving a specific rotational speed range, applying adequate axial force, and maintaining precise control over the welding parameters. The machine is designed to operate within a rotational speed range of 1500-2000 RPM, with an axial force of 10 kN and a torque of 47.74 Nm. These parameters are essential for generating frictional heat and ensuring proper material flow at the weld interface.

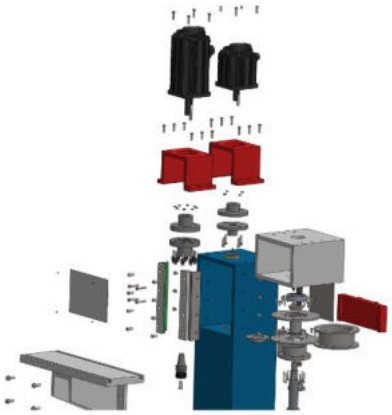

Figure 5, Exploded View of the Machine.

2.1.4. Tool Design

This FSSW tool design capitalizes on established equations derived from prior research, optimizing probe and shoulder diameters for exceptional performance in joining lightweight metals.

$$SD(mm) = 2.2 * Samplethickness(mm) + 7.3\,mm \quad (1)$$

$$PD(mm) = 0.8 * Samplethickness(mm) + 2.2\,mm \quad (2)$$

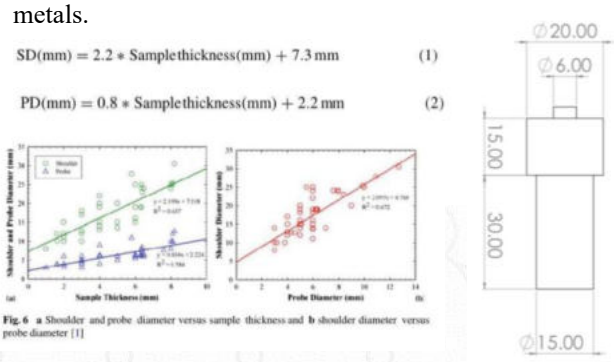

Fig. 6 a Shoulder and probe diameter versus sample thickness and b shoulder diameter versus probe diameter [1]

Figure 6, FSSW Tool Optimized Based on Research Findings.

3. Results and Discussion

The simulation results for the FSSW machine indicated that the design could handle the anticipated loads with a significant safety margin. The stress levels observed in the simulation were well below the ultimate tensile strength of the materials used, confirming the robustness and reliability of the design.

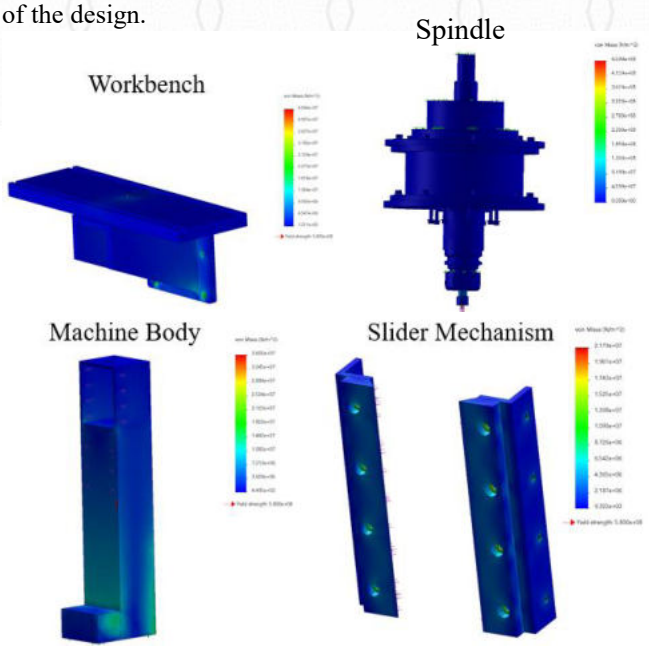

Figure 7, finite element analysis (FEA) for non-standard parts.

Finite element analysis (FEA) was conducted to evaluate the performance of critical components such as the spindle shaft, bearings, and slider mechanism under operational loads. The results demonstrated that the components could withstand the applied forces without deformation or failure, ensuring the structural integrity and longevity of the machine.

4. Conclusions

The project successfully developed a cost-effective FSSW machine capable of welding lightweight metals. Future work includes optimizing the machine's design to enhance performance further, reducing the weight of the machine components, and exploring additional welding techniques for broader applications. Integrating automatic feedback control systems and advanced end-effectors will improve the machine's versatility and operational capabilities.

References

[1] M. M. Z. Ahmed, M. M. E.-S. Seleman, I. Albaijan, and A. Abd El-Aty, "Microstructure, Texture, and Mechanical Properties of Friction Stir Spot-Welded AA5052-H32: Influence of Tool Rotation Rate," Materials, vol. 16, no. 9, May 2023.

[2] 1. S. G. Gb et al., "Improvements Relating to Friction Welding. Google Patents Ep0653265A2," 1994.

2. R. S. Mishra and Z. Y. Ma, "Friction stir welding and processing," Mater. Sci. Eng. R Reports, vol. 50, no. 1–2, pp. 1–78, 2005.

Electrochemical Corrosion Behavior of AMIG-Welded Stainless Steel

Nawaf Saad Alshmrani[1], Rashed Shujaa Aldosari[2], Hussein Alrobei[3], Rachid Djoudjou[4], Abousoufiane Ouis[5], Kamel Touileb[6]

Department of Mechanical Engineering, College of Engineering in Al-Kharj, Prince Sattam bin Abdulaziz University, Al-Kharj 11942, Saudi Arabia

[1] 439051770@std.psau.edu.sa; [2] 441050959@std.psau.edu.sa; [3] h.alrobei@psau.edu.sa; [4] r.djoudjou@psau.edu.sa; [5] a.ouis@psau.edu.sa; [6] k.touileb@psau.edu.sa

***Abstract*:** This project explored the corrosion behavior of stainless-steel welds in MIG-AMIG welds. Stainless steel samples were welded with either ER 70S-6 mild steel filler metals or ER 308 L stainless steel. Different fluxes were performed using different oxides (SiO_2, TiO_2, Fe_2O_3, Mn_2O_3, and Cr_2O_3) in the AMIG process. The voltage instrument combined with EC-Lab software made it easy to measure corrosion rates. The experiment aimed to compare corrosion resistance between different flows and determine the best flows among the tested samples.

Keywords: Corrosion Behaviour, Stainless Steel Welds, MIG-AMIG Welding, Filler Metals, Flux Oxides.

1. Introduction

Welding holds importance in the world (see Fig. 1), particularly in Saudi Arabia, due to the nation's vast industrial sectors, including petrochemicals, oil and gas, maritime, and construction industries. The harsh environmental conditions, such as high temperatures and salinity, pose significant challenges to material durability and integrity. Similarly, corrosion is particularly critical in Saudi Arabia because it directly impacts the infrastructure essential to these industries. Enhanced corrosion resistance of welds can lead to longer-lasting infrastructure, reduced maintenance costs, and fewer operational disruptions. By reducing the incidence of corrosion-related failures, significant cost savings can be achieved, contributing to the economic efficiency of industrial operations. This project aims to contribute to advancing welding technologies that meet the specific needs of Saudi Arabia's industrial landscape, ensuring better performance and extended service life of welded structures while minimizing economic losses due to corrosion.

Welding is essential in many industries, especially where stainless steel components need to be joined. The corrosion behavior of welds dramatically affects the durability and performance of the final product. In this scenario, this project aims to investigate the corrosion resistance of stainless-steel welds made using Metal Inert Gas (MIG) and Activated Metal Inert Gas (AMIG) welding techniques. Stainless steel samples were welded with two filler metals: ER 70S-6 mild steel and ER 308 L stainless steel.

Thus, the main goal of this experiment was to evaluate the corrosion resistance of different fluxes and identify which flux composition was the most effective among those tested. By identifying the best-performing flux, this research aims to enhance the durability of stainless-steel welds. This is especially advantageous for industries operating in harsh environmental conditions, such as those in Saudi Arabia, where improved corrosion resistance can lead to longer-lasting infrastructure and reduced maintenance costs.

Fig. 1. Welding Products Market size in 2023 [1].

2. Experimental Work

In this study, stainless steel grade 304 L was used. Two types of filler metal, ER 308 L and ER70S-6 (mild steel), were used. The samples were cut to the dimensions of 20 x 20 mm^2. For surface preparation, the samples were polished with 320, 400, 600, 800, and 1200 SiC (silicon carbide) paper and washed with water, followed by ethanol to remove excess moisture. The samples were then mounted in epoxy resin. All the electrochemical experiments were performed using a Biologic potentiostat SP-200 (Fig. 2), and the EC-lab software was used to analyze the results.

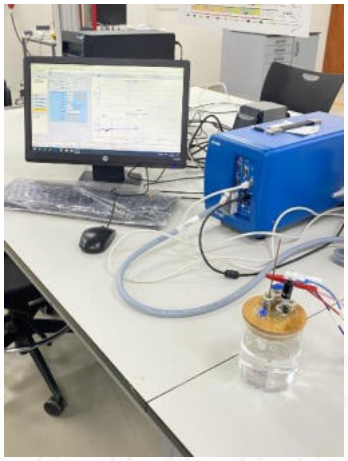

Fig. 2. Experimental set-up for the electrochemical experiments.

A potentiostat allows to change the potential of the metal sample in a controlled manner and measures the current that flows as a function of the potential. A three-electrode cell was

used to conduct the experiments using 300 ml of test solution. The working electrode (WE) was the epoxy resin mounted sample (with an exposed surface area of 2 cm^2), the reference electrode (RE) was a saturated calomel electrode (SCE), and the counter electrode was a platinum mesh.

2.1. Open-circuit potential (OCP).

Open-circuit potential (OCP or OCV, also called the resting potential, the equilibrium potential, or the corrosion potential) is the potential measured between the working electrode (WE) and the reference electrode (RE) when no current is passed. The measurement of an open-circuit potential is one of the more basic measurements of electrochemistry. The potential of metal immersed in an aqueous solution is a function of the fundamental reactivity of the metal and the oxidizing power of the aqueous solution. The setting used for this study is shown in Fig. 3.

The aim of these potential measurements is to determine the specimen's potential (working electrode) without affecting, in any way, electrochemical reactions on the surface of the specimen. It is necessary to make these potential measurements with respect to a stable reference electrode so that any changes in the measured potential can be associated with changes at the specimen/solution interface.

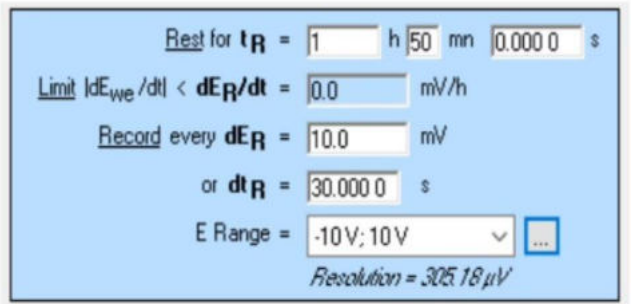

Fig. 3. OCP settings used for the system without chlorides.

2.2. Potentiodynamic polarization.

A potentiodynamic polarization scan allows one to acquire considerable information about the processes on the working electrode. Using this technique, the corrosion rate, susceptibility to pitting (a form of localized corrosion), passivity, and the cathodic behavior of an electrochemical system can be found. The settings used for performing potentiodynamic polarization are shown in Fig. 4.

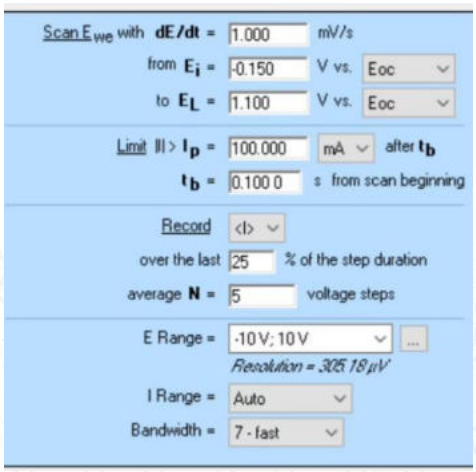

Fig. 4. OCP settings used for systems without chlorides.

3. Results and Discussion

Analysis of ER 308L filler metal and mild steel filler metal highlights a significant influence of flux type on the corrosion behavior of 304 SS welds in NaCl solution. For the ER 308L filler metal, welds made with SiO_2 flux showed the best corrosion rate value of (0.70349 mm/y), while for mild steel filler metal, the Fe_2O_3 flux had a lower corrosion rate of (0.0311 mm/y) and seemed to be the best in corrosion resistance compared to all samples. This indicates that the optimal approach to achieving corrosion-resistant welds in 304 SS depends on the specific filler metal used.

Fig. 5. (a)Potentiodynamic polarization graphs were obtained for base metals, and MIG and AMIG samples were welded with ER 308 L filler metal. (b) Potentiodynamic polarization graphs obtained for base metals MIG and AMIG samples welded with mild steel filler metal

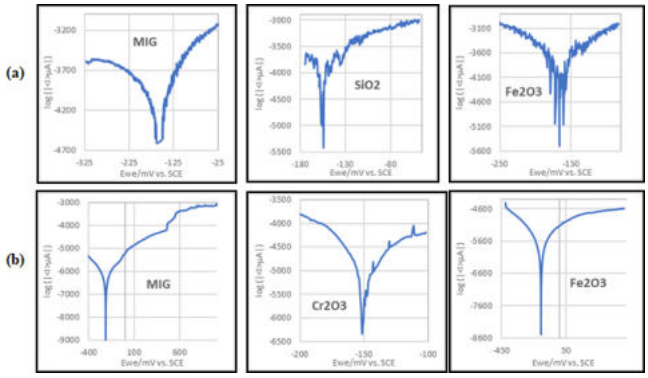

4. CONCLUSIONS

The study found that the corrosion behavior of 304 stainless steel welds in NaCl solution varied significantly based on the type of flux used. Welds made with ER 308L filler metal had the lowest corrosion rate (0.70349 mm/y) when using SiO2 flux. Conversely, mild steel filler with Fe2O3 flux demonstrated the highest corrosion resistance, with the lowest corrosion rate recorded at 0.0311 mm/y.

REFERENCES

[1] In-Depth Industry Outlook: Welding Products Market Size, Forecast (verifiedmarketresearch.com)

Design and Fabrication of a Soft Robot for Agri-food System Applications

Sultan A. Al-Otaibi[1], Khalid A. Al-Qahtani[2], Fehmi Najar[3]

Department of Mechanical Engineering, College of Engineering in Al-Kharj, Prince Sattam bin Abdulaziz University, Al-Kharj 11942, Saudi Arabia

[1] 438050040@std.psau.edu.sa; [2] 441051799@std.psau.edu.sa; [3] f.najar@psau.edu.sa

Abstract: A new approach to tackling issues in agriculture and food processing is using soft robots and biomimetic design for industrial agri-food systems. This work aims to design a soft robot tool with the specific purpose of manipulating and maneuvering products in the intricate and ever-changing settings found in the agri-food industry. The designed tool has three flexible fingers made of soft silicone materials. The control of these fingers is operated by pneumatic actuation. A suitable delta robot was also adapted and fabricated for the soft fingers. The preliminary tests showed a promising use of the robot for sensitive products in the agri-food sector.

Keywords: Soft robotics, hyperelastic material, pneumatic actuation, end-effector, delta robot manipulator.

1. INTRODUCTION

Nature's diversity often inspires breakthroughs in technical solutions, particularly in robotics, swarm robotics, autonomous operations, and safe human-machine interactions [1]. Several researchers are collaborating to design soft, lightweight robots that mimic human and/or animals' fluid movements to improve the energy efficiency and dexterity of the robots. On the other hand, soft robots are gaining attention for their adaptability, safety, deformability, mechanical strength, and cost-effective manufacturing [2].
Soft robotics technology can also help achieve the Sustainable Development Goals (SDGs) of the United Nations [3] by creating environmentally conscious, autonomous robots that run on renewable energy. For example, Giordano et al. explained how soft robotics can mitigate the adverse effects of climate change on human society and the environment by promoting adaptation, restoration, and remediation [4].

2. MATERIAL SELECTION

The material selection process is crucial for the soft robot end-effector since it will directly link to the robot's actuation, gripping and dexterity performance. Several constraints were considered for this selection; among these criteria, one can mention the shore of the material, the maximum allowable elongation, and the availability of the material.

2.1. Hyperelastic material

Due to the large deformations and large strains that can be observed while using these soft fingers, hyperelastic behavior should be considered. Materials such as silicone or acrylic and other elastomers are hyperelastic materials exhibiting large, almost purely elastic deformations. Depending on the targeted strain level, they can be modelled using several constitutive models. Neo-Hookean, Mooney-Rivlin, or Yeoh models are classically used for these materials [5].

2.2. Dragon Skin 30

After comparing several available materials, we selected the Dragon Skin 30 [6], a high-performance silicone rubber. Silicones are known for their excellent flexibility, tear strength, and long mold life.

Table 1. Mechanical properties of Dragon Skin 30 [6]

Tensile Strength (MPa)	Elongation (%)	Shore Hardness	Specific Volume (m^3/Kg)
3.45	364	30A	25.7

3. DESIGN ANALYSIS

The designed soft finger uses a pneumatic actuation through internal air chambers that enable its deformation. The chambers, shown in Figure 1, are partially separated by gaps that control the magnitude of its deformation characterized by a bending angle.

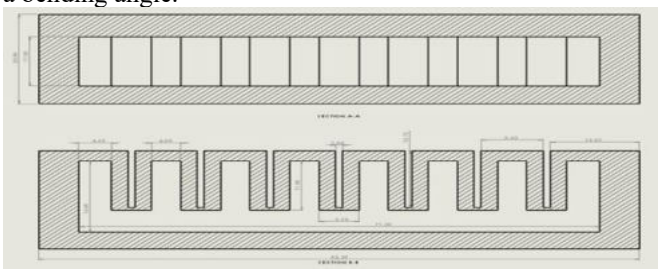

Fig. 1. Geometric dimension for the soft finger

A particular housing part is designed as the end-effector's main part, which fixes the fingers and ensures airflow entrance, as demonstrated in Figure 2.

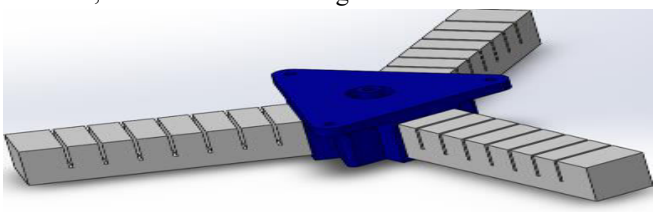

Fig. 2. End-effector CAD model

4. NUMERICAL SIMULATIONS

To test the designed shape of the finger, and due to the geometrical and material complexity, nonlinear static simulations are conducted using Ansys Mechanical. After testing the appropriate constitutive law for the selected hyperelastic material, curve fitting onto stress-strain unidirectional tensile test data found in the literature [5], the Yeoh second-order model is selected for our simulations. The

static structural module in Ansys imports the CAD design previously done in SolidWorks. The results showed that an appropriate finger deformation is obtained for air pressures around 70MPa, with a total deformation of around 11cm, as shown in Figure 3.

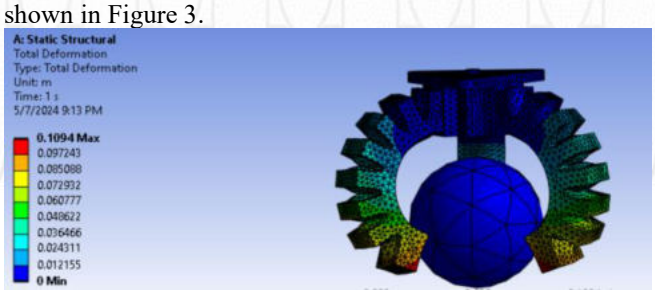

Fig. 3. End-effector total deformation in ANSYS

5. DELTA ROBOT MANIPULATOR

A particular kind of robot called a parallel manipulator is the delta robot, as depicted in Figure 4. Robots in this class have end-effectors powered by several underactuated parallel kinematic chains [7], which make them suitable for pick-and-place operations.

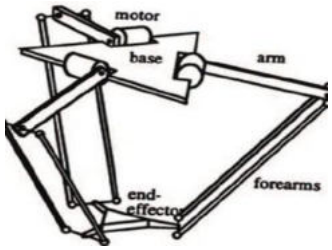

Fig. 4. Delta manipulator with 3 DOF [7]

6. FABRICATION

6.1 End-effector

We chose a mold fabrication technique for our soft gripper for its ease and cost-effectiveness. The principal mold is 3D printed for the outer finger shape. The corresponding CAD model is shown in Figure 5. Using an internal wax part, the air chamber is created by dissolving the wax after casting with a heat treatment.

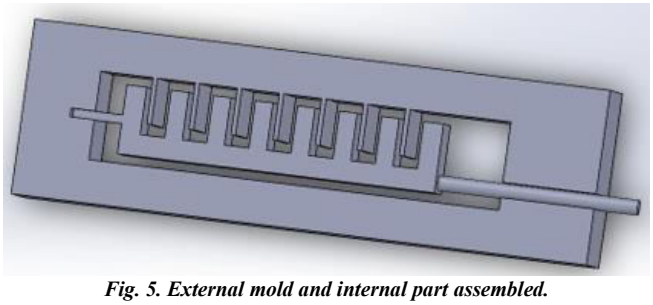

Fig. 5. External mold and internal part assembled.

Three fingers are manufactured and glued to the 3D-printed housing part. The assembly is connected to an air-pressure hose for testing purposes, as shown in Figure 6.

6.2 Delta Robot Manipulator

The manipulator is fabricated using laser-cutting sheet metal parts (Figure 7). The actuation uses three-step motors with an integrated planetary gearbox and is managed by an Arduino controller with a CNC-shield layer. G-code is used to define the end-effector trajectory.

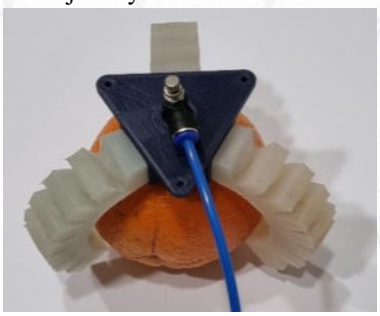

Fig. 6. End-effector prototype.

Fig. 7. Project prototype when assembly delta robot manipulator with end-effector

7. CONCLUSIONS

The eco-friendly soft robot was designed for agri-food industrial applications. Air-controlled soft material fingers are manufactured. A delta robot is used to control the fingers' motion for pick-and-place operations

REFERENCES

[1] Dong, X., Luo, X., Zhao, H., Qiao, C., Li, J., Yi, J., ... & Zeng, H. (2022). Recent advances in biomimetic soft robotics: fabrication approaches, driven strategies and applications. Soft Matter, 18(40), 7699-7734.

[2] Trimmer, B. (2013). Soft robots. Current Biology, 23(15), R639-R641.

[3] Fund, S. (2015). Sustainable development goals. Available at this link: https://www. un. org/sustainabledevelopment/inequality.

[4] Giordano, G., Murali Babu, S. P., & Mazzolai, B. (2023). Soft robotics towards sustainable development goals and climate actions. Frontiers in Robotics and AI, 10, 1116005.

[5] Melly, S. K., Liu, L., Liu, Y., & Leng, J. (2021). A review on material models for isotropic hyperelasticity. International Journal of Mechanical System Dynamics, 1(1), 71-88.

[6]www.smooth-on.com/products/dragon-skin-30/, accessed 20-03-2024.

[7] Hadfield, H., Wei, L., & Lasenby, J. (2020). The forward and inverse kinematics of a delta robot. In Advances in Computer Graphics: 37th Computer Graphics International Conference, CGI 2020, Geneva, Switzerland, October 20–23, 2020, Proceedings 37 (pp. 447-458). Springer International Publishing.

Design and Fabrication of 5-DOF, 3D Printed Industrial Robotic Arm for Pick and Place Application

Mohammed Abu Hajer[1], Abdullah Matar[2], Mukhtar Fatihu Hamza [3]

Department of Mechanical Engineering, College of Engineering in Al-Kharj, Prince Sattam bin Abdulaziz University, Al-Kharj 11942, Saudi Arabia

[1] 441052035@std.psau.edu.sa; [2] 441052015@std.psau.edu.sa; [3] mh.hamza@psau.edu.sa.

***Abstract*:** The design and fabrication of a 5-DOF, 3D-printed industrial robotic arm embodies a significant step forward in modern manufacturing, addressing critical challenges like labor shortages, high precision, and continuous operations. This project harnesses the precision of robotics and the flexibility of 3D printing, offering a cost-effective, adaptable, and precise solution that enhances efficiency and safety across various settings. The project's objectives included designing a prototype, fabricating parts using 3D printing, assembling the robotic arm, and conducting pick-and-place tests to ensure operational effectiveness. This report captures the journey from conceptualization to real-world application, showcasing the innovative integration of advanced technologies to revolutionize industrial tasks.

Keywords: design the prototype of 5-DOF, 3D-Printed Industrial Robotic Arm fabricated, assemble the parts, test & result the Robotic Arm, pick and place application.

1. Introduction

The progress in manufacturing technology highlights the need for flexible, accurate, and cost-effective solutions for industrial use. The 5-DOF robotic arm, a crucial part of this project, showcases these features by using the adaptable nature of 3D printing technology alongside the advanced capabilities of robotics. This combination allows for customized and quick design changes and ensures that tasks, incredibly moving and placing objects, are done with high precision and efficiency. This report covers the entire journey of Graduation Project 2, explaining the step-by-step design process, how materials and electronic parts were chosen and optimized, the hurdles faced while making and putting together the parts, and how these issues were tackled. A particular focus is on the innovative use of 3D printing to make parts, significantly lowering the cost and time needed for production while allowing for design flexibility. Additionally, the report details how the robotic arm was programmed and fine-tuned, showing how sensors and control systems were integrated to improve its accuracy and dependability [1].

2. Experimental Work

The project was conducted in several stages, including design, fabrication, and testing of the robotic arm components. The methodology section details the steps taken to achieve the project goals.

2.1 Design Parameters

The design process considered several key factors: functionality, end-effector selection, payload capacity, reach, axes, and mechanical design constraints [2].

2.1.1 Functionality

The robotic arm was designed to mimic human arm movements, allowing for picking, lifting, moving, lowering, and releasing objects. The design includes five parts and five joints, similar to a human arm, to perform complex tasks precisely.

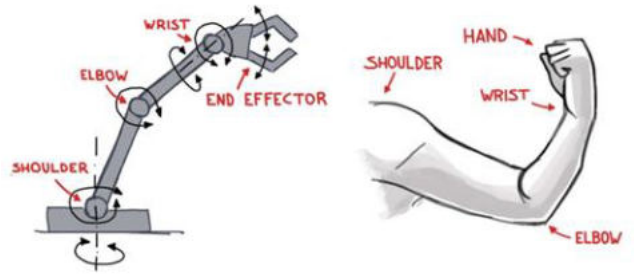

Fig. 1. Robotic Arm Functionality

2.1.2 End-Effector Selection

Various end effectors were considered, including suction cups, magnetic grippers, pneumatic grippers, and mechanical grippers. A mechanical gripper with rigid fingers was selected for its suitability for the intended tasks and simplicity of control.

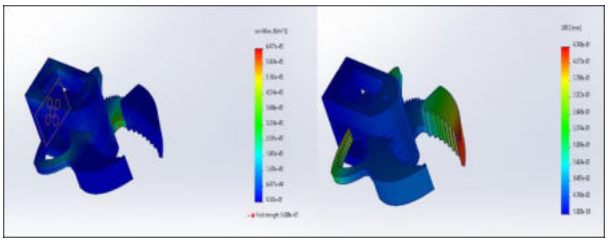

Fig. 2. Static Simulation for the Gripper.

2.1.3 Payload Capacity

The payload capacity was calculated using static equilibrium methods, ensuring the arm could handle the required loads without compromising stability .

2.1.4 Reach and Axes

The robotic arm was designed with five axes of motion, providing the necessary flexibility and range of motion to perform tasks within the designated workspace.

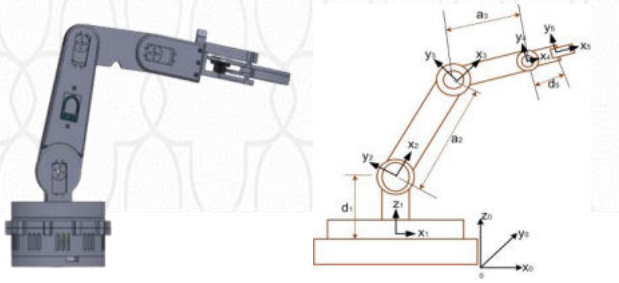

Fig. 3. CAD & Model of the 5-DOF Robotic Arm.

2.1.5 Mechanical Design Constraints

Constraints included size and dimensions, workspace, payload capacity, and end-effector requirements, ensuring the arm met all specified criteria.

Forward Kinematics **Inverse Kinematics**

$$^{A}P = {}^{0}T_{n}\,{}^{B}P \qquad \left({}^{0}A_{1}\right)^{-1}.\,{}^{0}A_{4} = {}^{1}A_{2}\,{}^{2}A_{3}\,{}^{3}A_{4}$$

2.2 Fabrication

The components of the robotic arm were fabricated using a 3D printer. PLA filament was chosen for its strength and flexibility. The printed parts were assembled to form the base, arm, and gripper subcomponents.

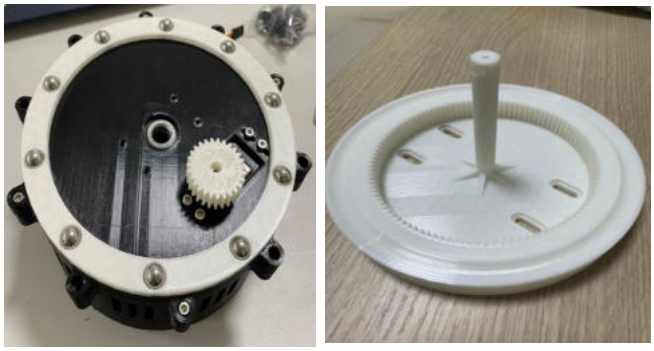

Fig. 4. Some 3D-printed Parts

2.3 Assembly and Control

The assembled robotic arm was controlled using an Arduino microcontroller, with servo motors providing precise movement. The control system allowed for manual open-loop control, adjusting the servo motors to achieve the desired joint angles[3].

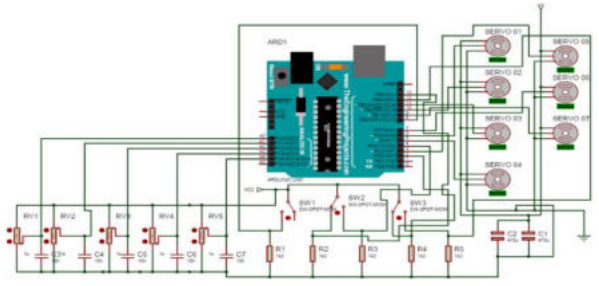

Fig. 5. Electrical Configuration of the Robot Wiring

3. Results and Discussion

The project implementation involved testing the robotic arm's joint accuracy and performing pick-and-place experiments. The accuracy of the joint angles was validated through systematic testing, showing minimal deviations from the commanded angles. The pick-and-place experiments demonstrated the arm's ability to handle different objects effectively, showcasing its flexibility and operational effectiveness .

Fig. 6. 5-DOF Robotic Arm 3D Printed Prototype

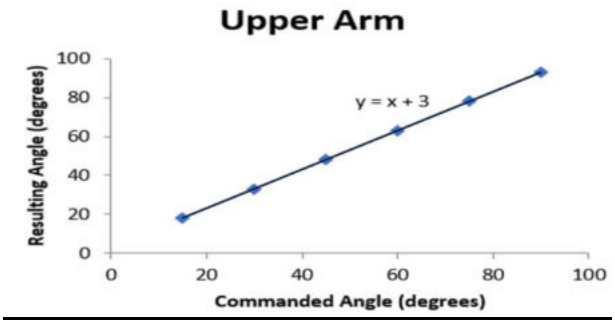

Fig. 7. Accuracy Test

4. CONCLUSIONS

The project successfully developed a 5-DOF, 3D-printed industrial robotic arm, demonstrating the potential of combining robotics with additive manufacturing. The robotic arm performed well in pick-and-place tasks, proving its feasibility for industrial applications. Future work includes optimizing the arm's design to reduce weight, implementing automatic feedback control, and exploring additional end-effectors for various applications.

REFERENCES

[1] J. Pires and A. Azar, "Robotic arm for additive manufacturing by fused deposition modeling," in 2018 13th International Conference on Robotics (ICR), pp. 1-6, IEEE, 2018.

[2] R. Ulrich and D. Eppinger, "Product design and development," McGraw-Hill, 2016.

[3]. Arduino Uno Rev3 [Online]. Available: https://store.arduino.cc/products/arduino-uno-rev3 (Accessed on May 13, 2024).

Design, Modelling, and Manufacturing of a Solar Dryer Prototype

Abdulaziz Al-Maymuni [1], Fahad Bin Lebdah[2], Lamjed Hadj-Taieb[3], Habib Ben Bacha[4]

Department of Mechanical Engineering, College of Engineering in Al-Kharj, Prince Sattam bin Abdulaziz University, Al-Kharj 11942, Saudi Arabia

[1] 439051146@std.psau.edu.sa; [2] 439051396@std.psau.edu.sa; [3] L.hadjtaieb@psau.edu.sa, [4] h.benbacha@psau.edu.sa ,

***Abstract*:** This study investigates the development of an indirect solar dryer, an eco-friendly solution for drying agricultural products. The first chapter provides a comprehensive background, emphasizing the need for sustainable drying methods in agricultural practices and reviewing existing drying technologies. The second chapter details the design phase, the theoretical underpinnings, and the engineering specifications for optimizing solar energy capture and heat transfer. In the third chapter, the focus shifts to the manufacturing process, the selection of materials describing the step-by-step construction, assembly of components, and quality control measures implemented to ensure reliability and efficiency. The final chapter presents the experiment results for specified products to see the temperature and relative humidity variation, the efficiency in moisture removal, and the quality preservation of dried products. Overall, the study confirms that the indirect solar dryer is a viable option for reducing post-harvest losses and enhancing the value of agricultural produce.

Keywords: Solar dryer, Indirect dryer, Solar collector, Drying chamber, PV panel.

1. Introduction

Solar drying technology represents a sustainable and eco-friendly approach to preserving various agricultural products, herbs, and commodities. By harnessing the sun's abundant energy, this method effectively removes moisture from goods, extending their shelf life while maintaining their nutritional integrity.

Solar drying involves using solar energy to facilitate the drying process, typically specially designed solar dryers [1]. As sunlight heats the drying chamber, air circulation facilitates moisture evaporation from the products, preserving them.

Furthermore, solar drying technology offers versatility across various industries and applications. Solar dryers can be adapted to suit a wide range of drying needs, from agricultural produce like fruits, vegetables, and grains to medicinal herbs, spices, and even textiles.

Solar dryers can be categorized into three main types [1]: direct, indirect, and specialized solar dryers. Each type operates based on different principles of solar energy collection and utilization.

This study focuses mainly on the following objectives:

- Develop a comprehensive background on the study.
- Choosing a solution for the study.
- Design all aspects of the solution.
- Manufacturing a prototype of the system.
- Perform experimental tests and data analysis.

2. Designing of Indirect Solar Dryer

2.1. Design Concept

The solar dryer considered in this work (Fig. 1) is a solar cabinet dryer for drying many products, such as tomatoes and grapes. The product is in trays made of wire mesh and plywood inside the drying chamber. The collector is placed at the sides of the cabinet and positioned in an open space to attract the sun's rays. To reduce heat loss, the collector is covered by Rock wool isolation. A fan forces air to enter through the open bottom end of the collector. Then, air is heated while it passes over the absorber. The warm air outlet of the collector is directed to the drying chamber. The heated air draws out the moisture from the product before exiting through the chimney.

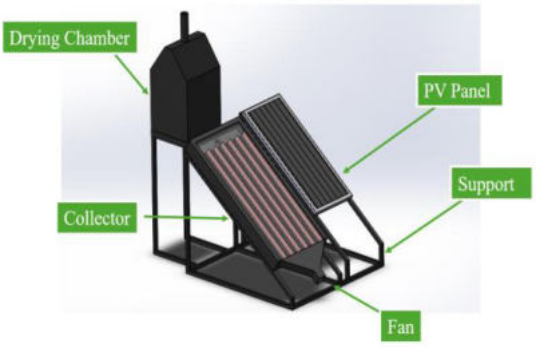

Figure 1: Indirect solar dryer design

2.2. Calculation

Design calculations involve determining the dimensions and specifications of the system components applied for tomatoes as the product. The mass of the product is $m_p = 3$ kg. Initial and final moistures are $M_i = 94\%$ and $M_f = 12.5\%$ respectively. The mass of water removed is

$$m_w = m_p \frac{(M_i - M_f)}{(100 - M_f)} = 2.79 \text{ kg} \quad (1)$$

The energy required to remove 2.79 kg of water

$$Q_t = m_p C_p \Delta T + \Delta H_{evp} = 2540.1 \text{ kJ/Kg} \quad (2)$$

By assuming an efficiency of 30% for the collector, the collector area is given by

$$A_c = \frac{m_w * Q_t}{I * \eta_{col} * 1000} = 1.592 \text{ m}^2 \quad (3)$$

The mass flow rate is

$$\dot{m} = \frac{Q}{C_p \Delta T} = 0.06 \text{ kg/s} \quad (4)$$

The height of the air column is obtained by [xx]:

$$H = \frac{\Delta P_T R}{g(\frac{1}{T_{amb}} - \frac{1}{T_{Dryer}})P_{atm}} = 0.66 \text{ m} \quad (5)$$

3. Manufacturing Process

This part provides detailed guidance on fabrication processes, construction techniques, and assembly procedures required for building functional solar dryers. We can assemble the prototype by putting all system components together, as shown in Fig. 2.

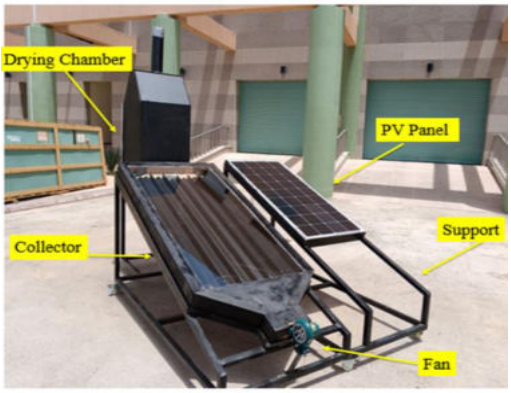

Figure 2: Solar dryer prototype

4. Experimental Work and Results

The experiment began on May 6th at 8:30 AM at the College of Engineering - Prince Sattam Bin Abdulaziz University. The system was put southeast between 8-11 AM, south between 11 AM – 3 PM, and west until 5:30 PM.

Fig. 3 shows the air temperature inside the solar collector. It increases by approximately 25°C as it heats the air while going through it. The maximum temperature of air reached is 64°C.

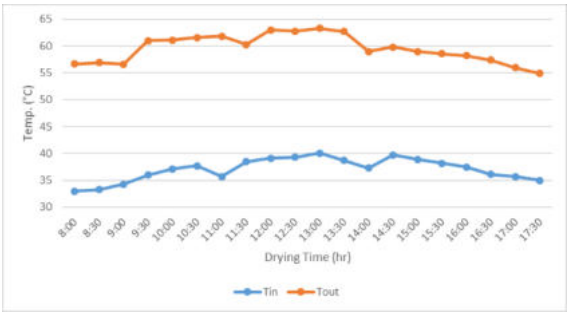

Figure 3: Air Temperature inside the collector

In the drying chamber, we can observe that the temperature is decreasing significantly (Fig. 4), which is due to the evaporation of water inside the crops, which led to the absorption of heat by the moisture. While drying and time passed, the temperature difference became smaller due to the crops' low moisture content.

At the beginning of the experiment, the relative humidity was high. Still, as the air continued entering the drying chamber, the relative humidity started to decrease (Fig. 5), and that was due to the moisture being removed from the crops. At the same time, there is no change in the ambient relative humidity.

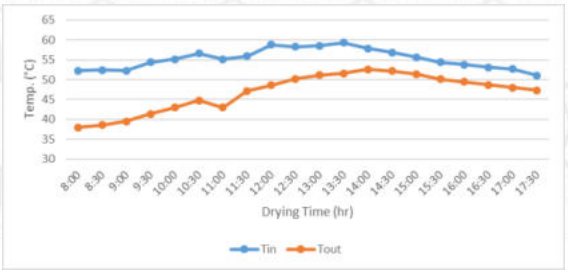

Figure 4: Air temperature inside the drying chamber

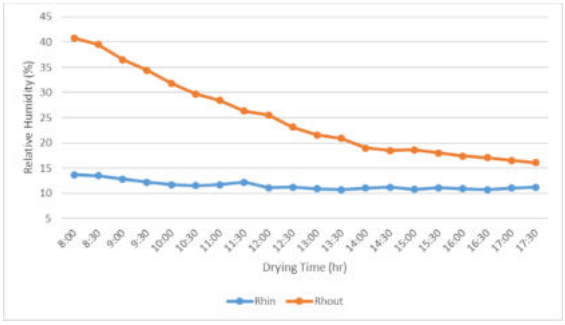

Figure 5: Relative humidity

After cutting the tomatoes into thin slices, they were spread evenly on the drying rack to increase the area of drying (Fig. 6a). We observe the difference in relative humidity when it reaches below 10% (Fig. 6b).

(a) **(b)**

Figure 6: Tomato slices (a) before drying, (b) after drying

5. Conclusion

This study successfully developed an indirect solar dryer that meets the objectives of energy efficiency, cost-effectiveness, and high performance. The systematic approach taken from background research to practical implementation and testing ensures that the dryer is scientifically sound and practically viable. This work lays a solid foundation for future research and development in solar drying technologies, potentially significantly impacting agricultural processing and food preservation in energy-scarce regions. The positive outcomes from this study suggest that further optimization and scaling could enhance the adoption and effectiveness of solar drying solutions globally.

References

[1] Prakash O., Kumar A. (2017). Solar drying technology. Part of the book series Green energy and technology. Springer Singapore.

Design and Fabrication of Indirect Evaporative Cooler

Mohamad Qosadi, Sulaiman Almoatham[1]

Department of Mechanical Engineering, College of Engineering in Al-Kharj, Prince Sattam bin Abdulaziz University, Al-Kharj 11942, Saudi Arabia

[1] s.almoatham@psau.edu.sa

Abstract: In this work, an indirect evaporative cooler was fabricated and tested indoors. The IEC was able to mitigate the increase in the relative humidity of the supply temperature. The supplied relative humidity was 44% instead of 99% for the direct evaporative cooler. However, the direct evaporative cooler achieves a lower supply temperature because the air stream directly hits the wetted pad.

Keywords: Evaporative cooler, IEC.

1. INTRODUCTION

Residential buildings consume 20% of global energy. Space heating and cooling applications account for 56% of this energy consumed in buildings. Improving living standards creates a need for cooling, especially in hot climate regions, which increases overall energy consumption and emissions. Most of the space cooling was done by vapor compression cycle devices. Because of the need for space cooling, upgrading or replacing the conventional vapor compression systems has significant energy-saving potential. One of the efficient alternatives to vapor compression is evaporative coolers. The main advantage of evaporative coolers over vapor compression is that they use water instead of refrigerants, lowering energy consumption. The evaporative coolers remove heat efficiently through the evaporation process.

2. OVERVIEW

Evaporative coolers are classified into direct evaporative and indirect evaporative coolers. In direct coolers, water evaporates into the airstream, consequently decreasing the dry bulb temperature of the air while adding moisture to it. On the other hand, in the indirect coolers, there are two air streams: one stream of air called primary air is cooled sensibly (without adding moisture) with a heat exchanger and this air cools the room. The secondary air carries away the heat energy from the primary air, and this secondary air is cooled by water and gets wet.

Indirect evaporative coolers (IEC) have the potential for various applications. This includes human or non-human thermal comfort. Most studies focused on using the IEC in buildings for space cooling. However, few studies have reported IEC's effectiveness in managing livestock and agricultural storage thermal comfort. **Figure *1*** shows various applications of the IEC.

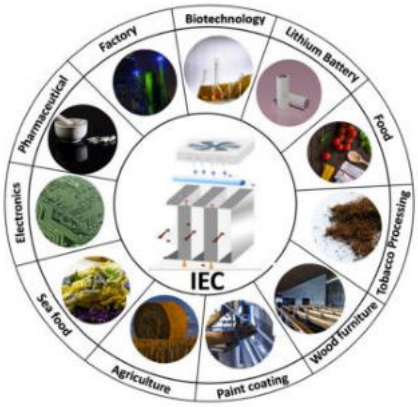

Figure 1. Applications of the IEC. (reprint from [1])

The working principle of the IEC is shown in **Figure *2***

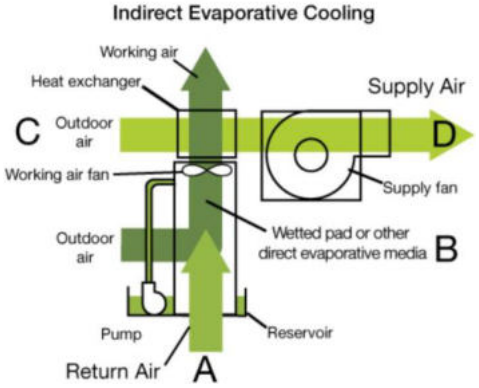

Figure 2. IEC working principle [3].

Several studies report an energy saving associated with the use of the IEC. For example, Maheshwari et al. conducted an analytical study utilizing field testing data from an Indirect Evaporative Cooler (IEC) unit in Kuwait. They compared the IEC unit's cooling performance and energy consumption to that of a conventional mechanical vapor compression refrigeration-based air conditioner with the same capacity. Results showed that in Kuwait's inland and coastal regions, the IEC unit achieved significant seasonal energy savings of 12,418 kWh and 6320 kWh, respectively, compared to the conventional air conditioner [2].

Despite the advantages of the IEC, the technology is far from being widely adopted for various reasons. The most significant factors impeding the IEC are the high dependency on the ambient air temperature, low-temperature reduction, and large geometric sizes. More research and development are needed to improve technological advances and market adoption.

3. MATHEMATICAL MODEL

Different indicative parameters are used to assess the performance of the IEC, such as the wet bulb effectiveness, cooling capacity, power consumption, energy efficiency, and evaporative cooler efficiency ratio (ECER).

The most popular approach is the wet bulb effectiveness, which considers the outlet temperature against the inlet wet bulb temperature as follows:

$$\varepsilon = \frac{T_{db\ in} - T_{db\ out}}{T_{db\ in} - T_{wb\ in}} \qquad (1)$$

Another parameter to assess the IEC is cooling capacity, which considers the enthalpy change between the inlet and the outlet of the IEC.

$$Q = c_p\, \rho V \left(T_{db_{in}} - T_{db_{out}}\right) \qquad (2)$$

4. EXPERIMENTAL WORK

The experiment was conducted on the designed prototype to evaluate the effectiveness of the IEC and compare it with the conventional direct evaporative cooler. Figure 3 and Figure 4 show the IEC prototype design. Moreover, the actual fabricated IEC is shown in Figure 5.

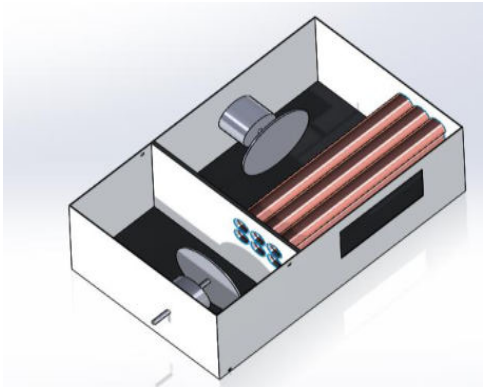

Figure 3. IEC final design

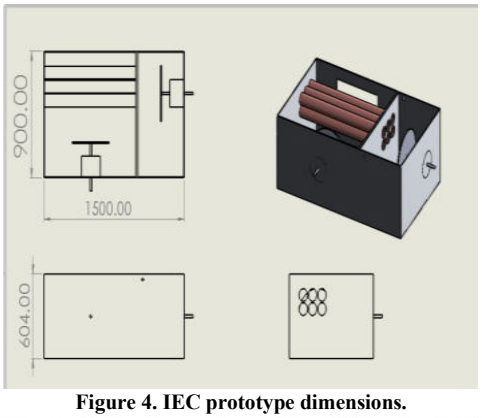

Figure 4. IEC prototype dimensions.

Figure 5. The top view of the IEC case shows the fan, heat exchanger, and wetted pad.

5. RESULTS

The test was conducted twice in an indoor climate. Each test lasted half an hour, and the readings were taken every 5 minutes. The indirect evaporative cooler reduced the temperature by 4 degrees, while the direct evaporative cooler reduced the temperature by 6 degrees. However, the IEC did a great job mitigating the increase in humidity. The supply air humidity was measured at 43% instead of 99%, as shown in Table 1 and Figure 6.

Table 1. Test results

T_{room} (°C) (inlet)	T_{supply} (°C) (direct)	T_{supply} (°C) (indirect)	dt (minutes)
26.5	22.7	24.5	5
	22	24.1	10
	22	24.1	15
	22	23.7	20
	21.1	23.7	25
	20.7	**22.8**	30
RH	**99%**	**43%**	

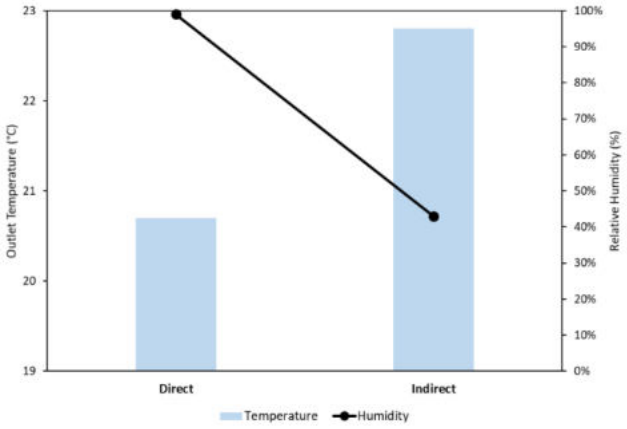

Figure 6. Comparison between direct and indirect evaporative cooler

4. CONCLUSIONS

Indirect evaporative cooler was fabricated and tested in an indoor environment. The IEC was able to mitigate the increase in the relative humidity of the supply temperature.

For future work, the performance of the IEC could be studied with the consideration of the following:

- The effect of the inlet water mass flow rate on the IEC.
- The effect of air volumetric flow rate from the primary and the secondary fan.

REFERENCES

[1] Sajjad et al., A review of recent advances in indirect evaporative cooling technology, International Communications in Heat and Mass Transfer, 2021.

[2] Duan et al., Indirect evaporative cooling: Past, present and future potentials, Renewable and Sustainable Energy Reviews, 2012.

[3] New Buildings Institute. Indirect evaporative coolers, 2014

Design and Development of a Green Hydrogen Production System

Salman Almalki[1], Faisal Alsaif[2], Ibrahim B. Mansir[3]

Department of Mechanical Engineering, College of Engineering in Al-Kharj, Prince Sattam bin Abdulaziz University, Al-Kharj 11942, Saudi Arabia

[1] 439051351@std.psau.edu.sa; [2] 439051878@std.psau.edu.sa; [3] i.balarabe@psau.edu.sa

***Abstract*:** Hydrogen as a clean energy carrier is being assessed for transition toward a sustainable energy future. The transition to a sustainable and low-carbon energy future faces a critical challenge in producing and integrating green hydrogen. Despite its immense potential to decarbonize various sectors, green hydrogen production remains hindered by several key obstacles. These obstacles include high production costs, inefficient electrolysis technologies, limited renewable energy integration, and inadequate infrastructure for storage and distribution. Saudi Arabia's vision 2030, is to produce about 1.2 million tons of green hydrogen and to supply 10% of the world's hydrogen needs. This project aimed to contribute to the national renewable energy program by designing a green hydrogen production system. The proposed system integrates water electrolysis technology, renewable energy sources, feed water quality, and materials for the system components. The design and implementation of the green hydrogen production system includes the design and/or selection of the required components such as electrolyzer module, green power unit, and water circulation system. Specifically, the system was designed to operate at a minimum capacity of more than 100ml/min. Remarkably, the system achieved a maximum hydrogen production rate of about 600 ml/min, showcasing its substantial output potential.

Keywords: Renewable energy; Green hydrogen; Water electrolysis; Sustainable energy.

1. Introduction

Many environmental issues, such as acid rain, stratospheric ozone depletion, and global warming, have been brought on by or are related to energy production, transformation, and use. This has led to a need for clean energy[1]. During the journey of transitioning to clean energy, a problem was found: the inability to fully exploit and store this obtained energy and use it for large and small usages. The pressing problem is to develop and implement innovative solutions that can address these challenges effectively, making green hydrogen a cost-competitive and scalable energy source[2]. So, here comes the role of hydrogen, which can preserve this clean energy produced in large quantities. But before that, the hydrogen production process needs to be clean. To achieve this, it is essential to advance research and development efforts in green hydrogen production methods, improve energy conversion efficiencies, reduce production costs, enhance electrolyzer technology, and expand renewable energy capacity. Additionally, building a comprehensive hydrogen infrastructure network and establishing regulatory frameworks to support its adoption are pivotal aspects of the solution[3]. The water electrolysis process has emerged as the most important method for producing hydrogen from renewable energy sources. Green hydrogen is a method for producing hydrogen with zero CO_2 emission through water electrolysis. So, this project aimed to design and develop a green hydrogen production system with a capacity of not less than 100ml/min.

2. System Development

The developed system consists of a photovoltaic panel, controller, and batteries for the power unit. In addition, an Alkaline water electrolyzer, water tank, pump, hydrogen and oxygen tanks, and separator tanks are shown in Figure 1. So, the electrolyzer where the water is split into hydrogen and oxygen, and the power unit supplies the electrolyzer with electricity.

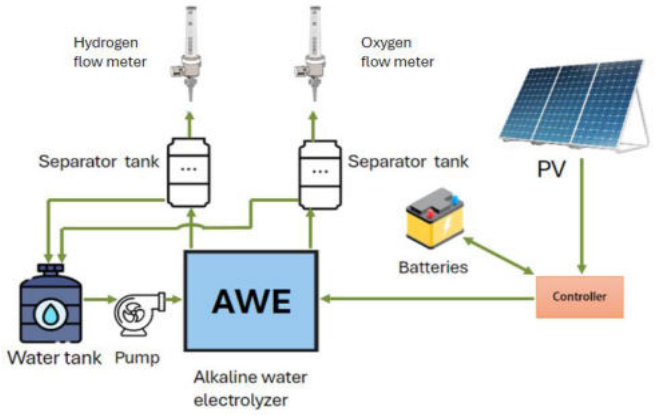

Fig. 1. The developed green hydrogen system (GHS) layout.

The power unit for the GHS consists of several components: a photovoltaic panel, batteries, controller, and cables. A stand-alone photovoltaic power system was designed based on the sizing of four main components: 1) load estimation, 2) battery capacity, 3) PV array, and 4) Controller selection. All the preceding components were meticulously designed, and their specifications are as follows: The total estimated load for this GHS was calculated to be 556.8 Wh. Golden plus 12V, 60Ah battery was selected. The selected PV module's properties are shown in Table 1. The selected controller is PWM with 20A and 12V.

Table 1: Power Capacity Demand

Parameters	Values
Total daily power consumption (Wh)	840
Perfect sun hours (h)	5
Derating factor (DF)	0.8
Battery round trip efficiency [BE] (%)	80
Power max. of panel (W)	200

.

The electrolyzer design consisted of the following parts: two base plates, electrolyte, anode, cathode separator, and sealing gasket. SolidWorks was used to design solid components. The dimensions of other parts were determined according to the dimensions of the base plates and the electrodes.

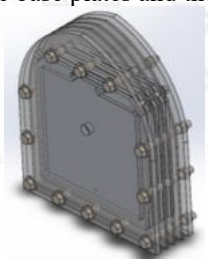

Fig.2. The design of the electrolyzer using SolidWorks.

3. Experimental Work

After assembling all system components, several tests were conducted on different materials, including stainless steel 316L, nickel, and titanium coated with 1µm platinum. The experiments were designed to evaluate the impact of varying sodium hydroxide (NaOH) concentrations on energy consumption, hydrogen production, and water temperature. The electrolyzer was tested using three different installation methods. In the first configuration, stainless steel 316L was installed on both cells. In the second configuration, both cells were equipped with nickel. The composition of the cells varied in the third setup, with each cell containing two pieces made of nickel and titanium coated with 1µm platinum. Figure 3 shows the experimental setup used.

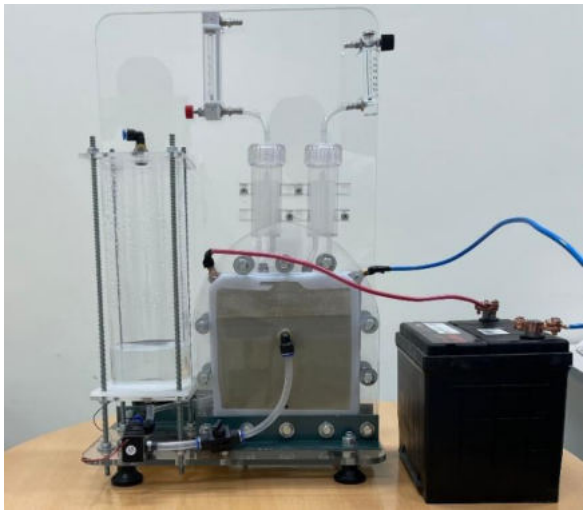

Fig.3. Experimental setup for the GHP system.

4. Results and Discussion

The results showed that increasing sodium hydroxide concentration results in higher hydrogen production across all configurations tested, as shown in Figure 4. However, this increase in production is accompanied by a simultaneous rise in energy consumption (Figure 5). The configuration consisting of Titanium Coated with 1µm platinum & Nickel and Nickel demonstrates notably greater hydrogen production than Stainless Steel 316L. Moreover, a slight variation is noted between Titanium Coated with 1µm platinum & Nickel and Nickel, with the former exhibiting superior production yields.

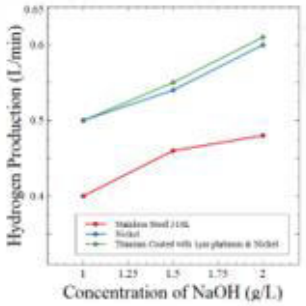

Fig.4. Effect of concentration on hydrogen production.

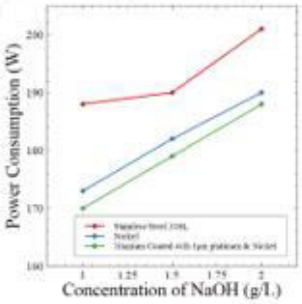

Fig.5. Effect of concentration on power consumption.

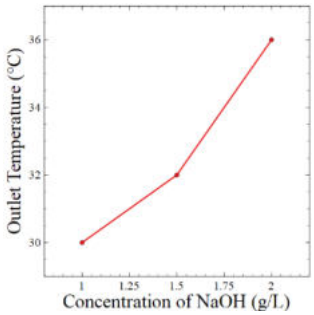

Fig.6. Effect of concentration on Temperature outlet

The findings shown in Figure 6 also reveal a direct correlation between the electrolyte concentration and the water temperature at the outlet. As the concentration increases, the outlet water temperature increases proportionally.

5. Conclusion

In conclusion, the designed and developed green hydrogen production system exhibits promising capabilities, operating efficiently for about 4 hours. The findings reveal a direct correlation between electrolyte concentration and hydrogen production across all materials tested. Notable differences in hydrogen production were observed among different materials, with Titanium coated with 1µm platinum and Nickel demonstrating superior yields compared to stainless steel 316L. Additionally, a marginal yet significant difference was noted between Titanium coated with 1µm platinum and Nickel and Nickel alone, with the former exhibiting higher production rates. Moreover, a direct relationship was established between sodium hydroxide concentration and outlet water temperature, with higher concentrations leading to elevated temperatures. The system achieved a maximum hydrogen production rate of 600 ml per minute.

References

[1] Cai, Q., Adjiman, C. S., & Brandon, N. P. (2014). Optimal control strategies for hydrogen production when coupling solid oxide electrolysers with intermittent renewable energies. *Journal of Power Sources*, 268, 212-224.

[2] Dincer, I. (2012). Green methods for hydrogen production. *International journal of hydrogen energy*, 37(2), 1954-1971.

[3] Santos, D. M., Sequeira, C. A., & Figueiredo, J. L. (2013). Hydrogen production by alkaline water electrolysis. Química Nova, 36, 1176-1193.

Mechanical Properties Evaluation of Helical Multi-wall Carbon Nanotube Enhanced Composite

Fahad Albuwardy[1], Abdulelah Alaskar[2], Ali Alamry[3], Mohammad Zaky[4], Hussein Alrobei[5]

Department of Mechanical Engineering, College of Engineering in Al-Kharj, Prince Sattam bin Abdulaziz University, Al-Kharj 11942, Saudi Arabia

[1] 439051001@std.psau.edu.sa; [2] 438050162@std.psau.edu.sa; [3] a.alamry@psau.edu.sa, [4] moh.ahmed@psau.edu.sa , [5] h.alrobei@psau.edu.sa

***Abstract*:** This project aims to fabricate an epoxy-reinforced Nanocomposite (HMWCNTs), study the effect of different concentrations, and evaluate its mechanical properties. The objectives of this project are nanocomposite preparation and fabrication, tension, impact, and hardness testing of the fabricated nanocomposite, and the identification of the fracture surface of the nanocomposite. In our approach, we used for the fabrication processes of HNWCNTs/epoxy a magnetic stirrer, an ultrasonic device, and a vacuum pump to enhance dispersion and ethanol to reduce agglomeration effect, then evaluate the mechanical properties of the composite material through tensile, impact and hardness. The results showed the highest tensile strength at a concentration of 2.75% with percentage of improvement 88.18 % of neat epoxy, an impact test at concentration 1.25% with percentage of improvement of 36.42 %, and a slightly increased hardness property.

Keywords: Nanocomposite, carbon nanotubes, epoxy, fabrication composite materials, mechanical testing.

1. Introduction

One of the most promising ways to improve the mechanical properties of composite materials is to incorporate carbon nanotubes (CNTs) into the matrix. CNTs are nanoscale structures with exceptional mechanical, electrical, and thermal properties, which can enhance the performance of composite materials. However, fabricating CNT to enhance composites requires achieving a uniform dispersion of CNTs in the matrix, which can affect the composite's interfacial bonding and mechanical properties. Moreover, many researchers have investigated how to fabricate and characterize these composites and found that the optimal CNT was 0.5 wt%, which improved the mechanical properties of the epoxy matrix. In this project, we aim to consider these challenges and fabricate epoxy/Helical Multi-Wall carbon nanotubes (HMWCNTs) with different concentration, which is 0.5 wt%, 1.25 wt%, 2 wt%, and 2.75 wt% and neat epoxy using an ultrasonic, magnetic stirring and vacuum pump to evaluating its mechanical properties.

We conducted several tests to evaluate the mechanical properties, including tensile, impact, and hardness tests, according to American Society for Testing and Materials (ASTM) standards for the specimens and scanning electron microscope (SEM) analysis. As shown in Fig. 1, we have manufactured several silicone rubber molds suitable for mechanical testing. We followed the ASTM D638 type 3 standard for tensile specimens, ASTM D2240 standard for hardness specimens, and Charpy standard for the impact test specimens [1][2][3].

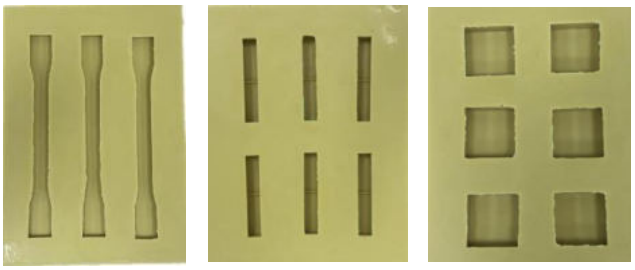

Fig. 1. Silicon rubber molds

The results of this project can provide valuable insights into Helical MWCNT's potential to enhance nanocomposites for various applications and contribute to the development of high-performance composite materials.

2. Experimental Work

Fabricated epoxy reinforced with HMWCNTs with different concentrations, which are 0.5 wt%, 1.25 wt%, 2 wt%, and 2.75 wt%, and neat epoxy using an ultrasonic and magnetic stirring to have good dispersion and ethanol solvent to reducing agglomeration effect and then evaluating its mechanical
properties.

2.1. Fabrication process

Epoxy resin was used to fabricate each compound with different proportions of HMWCNTs. In the initial processes, ultrasonic methods and a vacuum pump were used to achieve better dispersion and homogeneity in the magnetic stirrer. A certain amount of HMWCNT was mixed with ethanol using a magnetic stirrer at 600 rpm for 30 min. Then, the required amount of epoxy resin was added to the HMWCNTs/ethanol mixture and stirred manually for 10 min and at 800 rpm using a magnetic stirrer for 10 min. Ultrasound was then performed for 30 minutes at 20 kHz. Then again use a magnetic stirrer at 800 rpm for 60 minutes or until the ethanol evaporates at 80 °C. Ultrasound was then performed again for 30 minutes at 20 kHz at 60°C. Next, use a vacuum pump to remove air

bubbles from the mixture for 30 minutes. After that, a certain amount of hardener was added in a ratio of 1:2 to the mixture. Finally, the mixture was poured continuously into the mold to manufacture 5 samples of epoxy nanocomposites, as shown in Fig. 2. Samples were processed at room temperature for 48 hours. We produced six specimens for each mechanical test sample, as illustrated in Fig. 3.

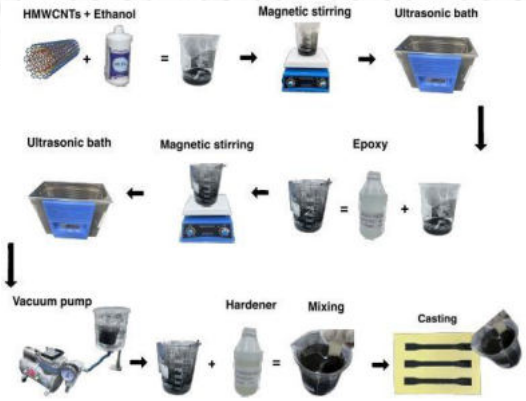

Fig. 2. Fabrication process.

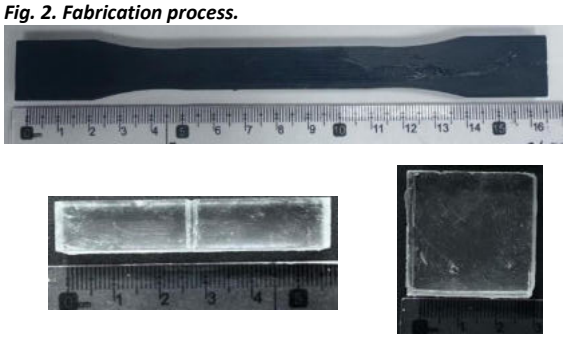

Fig. 3. Fabricated sample.

2.2. Mechanical testing.

Mechanical tests were used, including tensile, impact, hardness, and scanning electron microscope (SEM) analysis. Using a universal tensile testing machine (WDW-50 JINAN TESTING EQUIPMENT IE CORPORATION), tensile testing was performed at a 5 mm/min loading speed. The impact testing was conducted at SABIC using a Zwick Roell impact testing machine model H1T50P, manufactured by a German company. A digital durometer was used to perform the Shore D hardness test.

3. Results and Discussion

Epoxy reinforced with 0.5%,1.25%,2% and 2.75% of HMWCNTs. The samples were prepared with six specimens for each test. As shown in Fig. 4, the tensile test results indicate that increasing the HMWCNTs concentration significantly improves the tensile strength of the Nanocomposite. The first concentration shows a significant increase in stress with a decrease in strain, leading to a 51.12% improvement in stress. The second and third concentrations enhance tensile strength, resulting in percentage improvements of 57.19% and 74.23% of the epoxy, respectively. However, the strain also varies among the concentrations. The fourth concentration shows the highest stress value but has a higher strain as well, leading to a significant improvement of 88.18% in the tensile strength of the epoxy.

All concentrations show improvement for both impact strength and hardness, as illustrated in Fig. 5. The highest increase in impact strength is at 1.25% HMWCNTs, with a 36.42% improvement over neat epoxy. The greatest increase in hardness is at 2.75% HMWCNTs, but the improvement is slight.

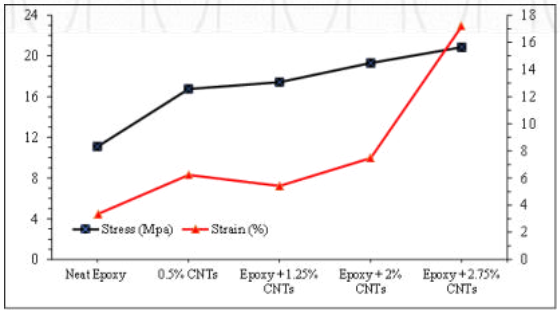

Fig. 4. Stress and strain of epoxy and epoxy/HMWCNTs.

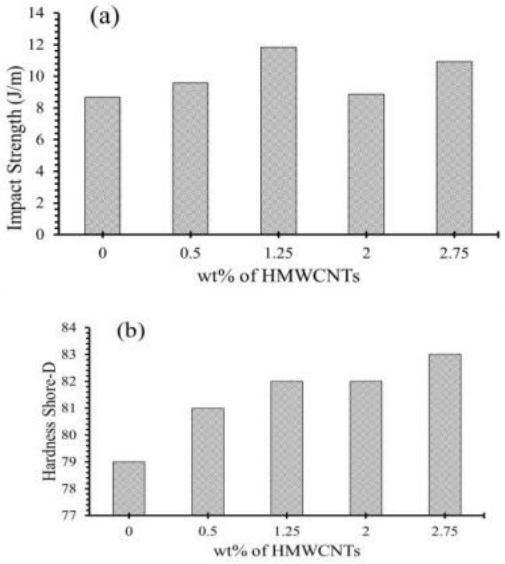

Fig. 5. Impact and Hardness properties of HMWCNTs/epoxy Nanocomposite: (a) Impact Strength and (b) Hardness Shore-D.

CONCLUSIONS

We studied the effect of different concentrations, and their mechanical properties were evaluated. It also became clear that the tensile strength increased at a concentration of 2.75%. The improvement in the impact test was for the 1.25% concentration, and the improvement in the hardness test was slight.

REFERENCES

[1] I. Cantox, “ASTM D638 vs ASTM D3039 Testing for Tensile Properties.” [Online]. Available: http://www.intertek.com/polymers/composites/nadcap/

[2] Mahmood Hisham Shubbak, “Material Science Laboratory- impact test, 2008-2009”.

[3] “ASM International, Hardness Testing, 2nd Edition, 06671G.”.

Numerical Simulation of Advanced Energy Materials Applications

Omar A. Al-Malki[1], Muhanna M. Al-Dosari[2], Abdulkarim A. Aldawish[3], Abdullah H. Alshehri[4], Mutabe S. Aljaghtham[5]

Department of Mechanical Engineering, College of Engineering in Al-Kharj, Prince Sattam bin Abdulaziz University, Al-Kharj 11942, Saudi Arabia

[1] 439051092@std.psau.edu.sa; [2] 438050033@std.psau.edu.sa; [3] 439051139@std.psau.edu.sa; [4] abd.alshehri@psau.edu.sa; [5] m.aljaghtham@psau.edu.sa

Abstract: The project aims to develop a simulation model using numerical methods in COMSOL to analyze the optical properties, conducting tests on the optical properties of Titanium Dioxide (TiO2). Based on the obtained results, the optimal thickness of the material can be determined depending on the application. It was observed that increasing the thickness leads to a decrease in transmittance and an increase in reflectance and absorption within the wavelength range of 200 to 370 nanometers. The I-V curve of solar cell application was generated for three layers: the first layer, AlSb, with a thickness of 200 nanometers; the second layer, AgInTe2, with a thickness of 600 nanometers as an absorptive and generating layer; and the last layer, BaSi2, as a gap carrier layer with a thickness of 200 nanometers.

Keywords: Solar cell, energy materials application, optical properties, numerical simulation.

1. INTRODUCTION

Advanced energy materials is a term given to materials that are used in developing and improving various technologies for generating, storing, and using energy. This includes a wide range of materials, such as solar materials, electrical and magnetic materials, advanced chemical and biological materials, reflective and heat-conducting materials, materials used in battery and storage technology, photocatalysts, and nanomaterials. Thin films are one of the essential components of many devices and are materials that are small in thickness. Thin films are a material or several solid materials placed on a substrate's surface whose physical and chemical properties are to be improved by specific means. They consist of a thickness ranging from 1nm-1µm [1]. Thickness is vital in thin films and is an essential factor affecting the optical, electrical, thermal properties, etc [2]. Thin films are used in many fields, such as electronics, power, optics, sensors, solar energy, germ protection, and other applications. Thin films can be made of metals, oxides, metals with oxides, polymers, or carbon compounds [3].

2. OPTICAL SIMULATION

Optical properties is a term that describes the behavior of a material when exposed to electromagnetic radiation (light). Light has properties when it falls on a surface: part of it is transmitted, part is reflected, and the material absorbs part; electromagnetic radiation appears as the only one capable of reflection, absorption, and transmission and is visible to the human eye. Light transmission occurs when an incident ray strikes a transparent or translucent object where the light can travel. The absorption of light occurs when the light falls on the body and then turns into energy. The electrons can move to higher energy levels when they absorb this energy. Reflection occurs when light strikes a surface and is reflected directly from it.

3. MATERIAL SELECTION

Air, TiO2 (Titanium dioxide), and substrate are the materials chosen for simulation for the thin films. The properties used in the simulation were obtained from the COMSOL library.

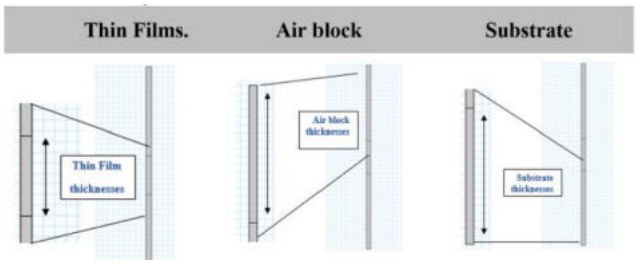

Fig. 1. Schematic of device layers.

4. DESIGN ANALYSIS OF THE 3D MODEL

A three-dimensional simulation model is a mathematical representation of a system, process, or phenomenon used to simulate or mimic real-world behavior. Simulation models are commonly used in various fields, from engineering to social sciences. These models can range from simple to highly complex and can be developed using various software tools and techniques.

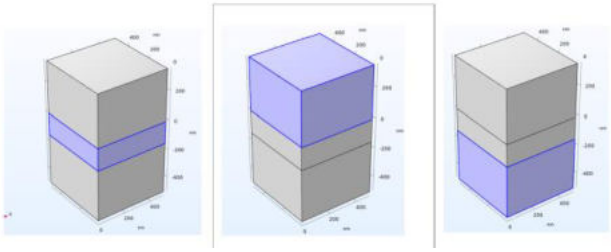

Fig. 2. Geometric dimensions of physical models

5. SOLAR CELL APPLICATION

The efficiency rate at which solar cells convert light into electricity varies according to the type of semiconductor material and the solar cell technology used. The efficiency of

commercial solar modules was less than 10% in the mid-eighties, rose to about 15% by 2015, and is now approaching 25% for modern high-tech modules. Multi-junction solar cells are an advanced technology that converts solar energy into electrical energy. These cells have a multi-layer design, where each layer absorbs a specific range of solar wavelengths.

6. RESULTS

In this section of the results, the thickness of each layer was individually varied while keeping the other thicknesses constant to examine the effect that occurs in each layer due to changes in its thickness and its impact on the overall cell performance. Firstly, the thickness of the first layer, AlSb, was changed to various thicknesses from 100 nanometers to 600 nanometers while keeping the other thicknesses constant. Also, the power and I-V curve is obtained for optimal thickness.

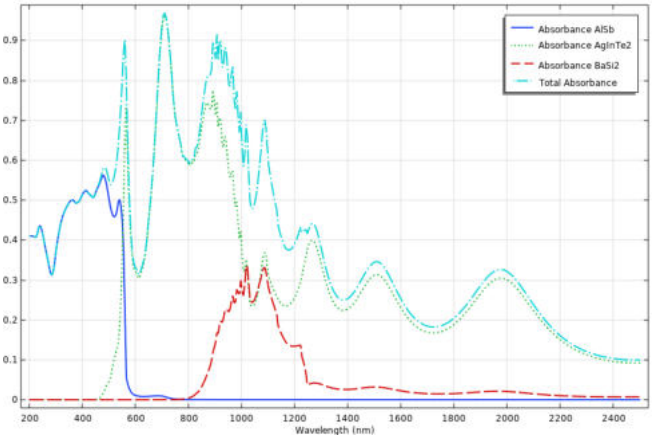

Fig. 3. Absorbance for all layers graph depending on the change in wavelength

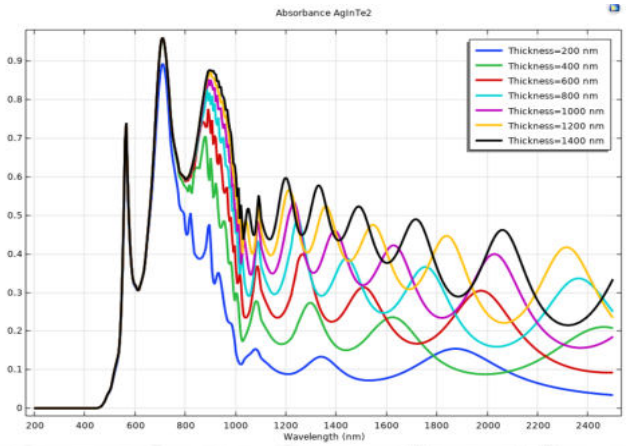

Fig. 4. Total absorbance for different thicknesses of AlSb.

4. CONCLUSIONS

The study presents two simulation models built on the COMSOL Multiphysics program, relying on numerical analysis of optical properties to enhance the performance of solar cells. The first model focuses on exploring optical characteristics and the impact of thickness, testing titanium dioxide for its absorptive, transmissive, and reflective properties. Various thicknesses were identified to understand the thickness effect on optical properties and determine the spectral gap of titanium dioxide at variable thicknesses, contributing to the understanding of thickness impact on the spectral gap. An I-V curve was created for three layers: the first layer, AlSb, with a thickness of 200 nanometers; the second layer, AgInTe2, with a thickness of 600 nanometers as an absorptive and generating layer; and the last layer, BaSi2, as a gap carrier layer with a thickness of 200 nanometers. The solar cell efficiency was determined to be 5.96%.

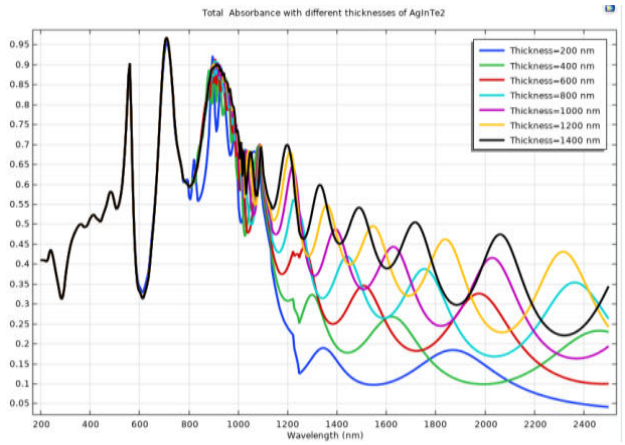

Fig. 5. Total absorbance for different thicknesses of AgInTe2.

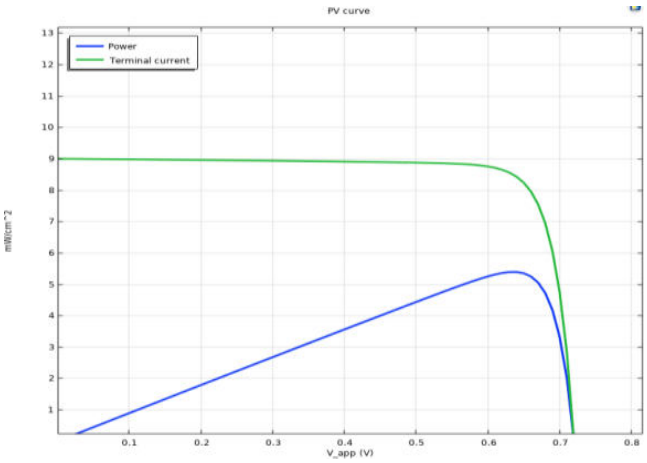

Fig. 6. I-V curve and power of the solar cell.

REFERENCES

[1] *Thin Films And Their Uses | Industry Outlook*. (n.d.).Retrieved May 25, 2023, from https://www.theindustryoutlook.com/manufacturing/news/6-types-of-thin-films-and-their-uses-nwid-3769.html

[2] Lou, B., Chen, W., Diyatmika, W., Lu, J., Chen-Te, C., Chen, P., & Lee, J. (2022). High power impulse magnetron sputtering (HiPIMS) for fabricating antimicrobial and transparent TiO2 thin films. *Current Opinion in Chemical Engineering*, *36*, 100782. Retrieved May 25, 2023

[3] Jian, D. (n.d.). Thin Film Sensors vs. Traditional Sensors - A Comparison. *www.linkedin.com*. Retrieved May 25, 2023,